



# QUALITY INFORMATION DOCUMENT

## QUALITY INFORMATION DOCUMENT For Global Ocean Reanalysis Products GLOBAL\_REANALYSIS\_PHY\_001\_030

**Issue:** 1.5

**Contributors:** Marie Drévillon, Jean-Michel Lellouche, Charly Régnier, Gilles Garric, Clément Bricaud, Olga Hernandez, Romain Bourdallé-Badie

**Approval Date by Quality Assurance Review Group : 07/12/2021**

## **CHANGE RECORD**

<b>Issue</b>	<b>Date</b>	<b>§</b>	<b>Description of Change</b>	<b>Author</b>	<b>Checked By</b>
1.0	18 January 2018	all	First version of document		
1.1	24 april 2018	title	Correct number of product in the document	Yann Drillet	
1.3	11 december 2020	NB	Add note to describe the switch to ERA5 forcing	Romain Bourdallé-Badie	
1.4	13/01/2021	all	Add dataset global-reanalysis-phy-001-030-monthly-climatology	Marie Drévillon	Marie Drévillon
1.5	07/12/2021		Time extension	Romain Bourdallé-Badie	Marie Drévillon

## **TABLE OF CONTENTS**

<b>I EXECUTIVE SUMMARY.....</b>	<b>5</b>
<b>I.1 Products covered by this document .....</b>	<b>5</b>
<b>I.2 Summary of the results .....</b>	<b>6</b>
<b>I.2.1 Temperature.....</b>	<b>6</b>
<b>I.2.2 Salinity .....</b>	<b>7</b>
<b>I.2.3 Ocean currents .....</b>	<b>7</b>
<b>I.2.4 Sea level.....</b>	<b>7</b>
<b>I.2.5 Transports .....</b>	<b>7</b>
<b>I.2.6 Sea Ice concentration.....</b>	<b>8</b>
<b>I.3 Estimated Accuracy Number .....</b>	<b>9</b>
<b>II Production Subsystem description .....</b>	<b>10</b>
<b>II.1 GLORYS12V1 reanalysis (001_030) .....</b>	<b>10</b>
<b>III Validation framework .....</b>	<b>15</b>
<b>IV Validation results of GLORYS12V1 .....</b>	<b>16</b>
<b>IV.1 Temperature .....</b>	<b>16</b>
<b>IV.1.1 T-CLASS1-T3D-MEAN .....</b>	<b>16</b>
<b>IV.1.2 T-CLASS1-SST-MEAN.....</b>	<b>17</b>
<b>IV.1.3 T-CLASS1-SST-TREND.....</b>	<b>18</b>
<b>IV.1.4 T-CLASS2-MOORINGS.....</b>	<b>19</b>
<b>IV.1.5 T-CLASS3-SST_QNET_MEAN.....</b>	<b>21</b>
<b>IV.1.6 T-CLASS3-HC_LAYER .....</b>	<b>21</b>
<b>IV.1.7 T-CLASS4-LAYER .....</b>	<b>22</b>
<b>IV.1.7.1 Timeseries .....</b>	<b>22</b>
<b>IV.1.7.2 2D Maps.....</b>	<b>23</b>
<b>IV.1.8 T-DA-INNO-STAT .....</b>	<b>25</b>
<b>IV.2 Salinity .....</b>	<b>27</b>
<b>IV.2.1 S-CLASS1-S3D_MEAN .....</b>	<b>27</b>
<b>IV.2.2 S-CLASS1-SSS-TREND.....</b>	<b>28</b>
<b>IV.2.3 S-CLASS2-MOORINGS .....</b>	<b>28</b>
<b>IV.2.4 S-CLASS3-SSS_SFW_2DMEAN .....</b>	<b>30</b>
<b>IV.2.5 S-CLASS3-SC_LAYER.....</b>	<b>31</b>
<b>IV.2.6 S-CLASS4-LAYER.....</b>	<b>32</b>
<b>IV.2.6.1 Timeseries .....</b>	<b>32</b>
<b>IV.2.6.2 2D Maps.....</b>	<b>33</b>
<b>IV.2.7 S-DA-INNO-STAT.....</b>	<b>35</b>
<b>IV.3 Currents .....</b>	<b>36</b>
<b>IV.3.1 UV-CLASS1-15m_MEAN.....</b>	<b>36</b>
<b>IV.3.2 UV-CLASS2-MOORINGS.....</b>	<b>37</b>
<b>IV.3.3 UV-CLASS2-MKE_1000m .....</b>	<b>39</b>
<b>IV.4 Sea level .....</b>	<b>39</b>
<b>IV.4.1 SL-CLASS3-2DMEAN .....</b>	<b>39</b>
<b>IV.4.2 SL-CLASS4 .....</b>	<b>40</b>
<b>IV.4.3 SL-DA-INNO_STAT .....</b>	<b>40</b>
<b>IV.5 Transports .....</b>	<b>41</b>
<b>IV.5.1 UV-CLASS3-VOL_TRANSPI.....</b>	<b>41</b>
<b>IV.5.2 UV-CLASS3-AMOC .....</b>	<b>42</b>
<b>IV.5.3 T-CLASS3-MHT .....</b>	<b>42</b>
<b>IV.6 Sea Ice.....</b>	<b>44</b>
<b>IV.6.1 SI-CLASS1-CONC_MEAN .....</b>	<b>44</b>
<b>IV.6.2 SI-CLASS1-CONC_EXTREME .....</b>	<b>46</b>

IV.6.3	<b>SI-CLASS3-EXTENT.....</b>	47
IV.6.4	<b>SI-CLASS3-EXTENT_ANO.....</b>	47
IV.6.5	<b>SI-CLASS3-VOL .....</b>	48
IV.6.6	<b>SI-CLASS3-VOL_ANO.....</b>	48
IV.6.7	<b>SI-CONC-DA-INNO-STAT .....</b>	49
<b>V</b>	<b><i>System's Noticeable events, outages or changes .....</i></b>	<b>50</b>
<b>VI</b>	<b><i>Quality changes since previous version.....</i></b>	<b>51</b>
<b>VII</b>	<b><i>References .....</i></b>	<b>52</b>

## I EXECUTIVE SUMMARY

---

### I.1 Products covered by this document

The product assessed in this document is referenced as:

**GLOBAL-REANALYSIS-PHY-001-030** for Global Ocean Physics Reanalysis system product.

The goal of the CMEMS global ocean reanalysis is to provide a eddy resolving (1/12°) global ocean simulation, covering the recent period during which altimeter data are available (period starting with the launch of TOPEX POSEIDON and ERS-1 satellites early in the nineties), constrained by assimilation of observations and describing the space-time evolution of the following variables:

- \* sea\_surface\_height\_above\_geoid
- \* sea\_water\_potential\_temperature
- \* sea\_water\_salinity
- \* sea\_water\_x\_velocity
- \* sea\_water\_y\_velocity
- \* sea\_ice\_area\_fraction
- \* sea\_ice\_thickness
- \* sea\_ice\_x\_velocity
- \* sea\_ice\_y\_velocity

These reanalyses are built to be as close as possible to the observations (i.e. realistic) and in agreement with the model physics. It covers the “altimetry era” (namely 1<sup>st</sup> of January 1993 until **30 May 2020** for 001\_030). The numerical products available for users are daily averages and monthly mean averages describing the ocean from surface to bottom (5900 m).

The product GLOBALREANALYSISPHY-001-030 consists of a global ocean reanalyses datasets at 1/12° horizontal resolution. The product is distributed on a regular 1/12° grid. See the Product User Manual for more details about the grid.

The table below (Table 1) synthesizes the different data sets of the global ocean physical reanalysis products:

Product Name	Product origin	Production Unit	Data set	Kind of data set
GLOBAL_REANALYSIS_PHY_001_030	GLORYS12 V1	GLO-MERCATOR-TOULOUSE-FR	global-reanalysis-phy-001-030-monthly-climatology-t global-reanalysis-phy-001-030-monthly-climatology-s global-reanalysis-phy-001-030-monthly-climatology-u-v global-reanalysis-phy-001-030-monthly-climatology-ssh global-reanalysis-phy-001-030-monthly-climatology-iceglobal-reanalysis-phy-001-030-monthly-t global-reanalysis-phy-001-030-monthly-s global-reanalysis-phy-001-030-monthly-u-v global-reanalysis-phy-001-030-monthly-ssh global-reanalysis-phy-001-030-monthly-ice dataset-global-reanalysis-phy-001-027-ran-fr-glorys12v1-coordinates global-reanalysis-phy-001-030-daily-t global-reanalysis-phy-001-030-daily-s global-reanalysis-phy-001-030-daily-u-v global-reanalysis-phy-001-030-daily-ssh global-reanalysis-phy-001-030-daily-ice	reanalysis

Table1: Overview of **GLOBAL\_REANALYSIS\_PHY\_001\_030** product.

## I.2 Summary of the results

### I.2.1 Temperature

GLORYS12V1 reanalysis has weak regional biases (less than 0.4 °C) in temperature with respect to the World Ocean Atlas 2013 climatology and in-situ data (less than 0.1°C on global average with respect to in-situ temperatures). The largest biases occur in the [50 m-100 m] layer and in the northern Atlantic and Southern oceans.

The global mean sea surface temperature (SST hereafter) is close to the observations with a weak (warm) misfit of less than 0.1°C all along the reanalysis. The global positive SST linear trend is highly consistent with AVHRR data. The global mean surface net heat flux is weakly negative (- 0.7 W.m<sup>2</sup>).

Along the equator, temperature profiles are very consistent with observations with RMSD (Root mean square errors) generally smaller than 0.4°C in the water column, apart from the [50 m-200 m] layers where the RMSD can intermittently reaches 1.2°C in the Indian Ocean. Correlations with equatorial moorings also decrease with depth.

The heat content constantly increases with time until 2011. Since 2011, the heat content may have stabilised. Only the deeper layers (below 2000 m depth) show a constant cooling.

The thermal structure largely improves with the deployment of Argo buoys (after 2002), mainly in the upper layers (depth < 300 m) with a (cold) bias close to 0°C and RMSD against all the in-situ

observations less than 1°C. The RMSD also decreases with time in accordance with the observations network density.

### **I.2.2 *Salinity***

The sea surface salinity (SSS hereafter) is generally fresher than both the climatology with regional biases of less than 0.2 psu, except in the Arctic where larger biases appear. The global average of salinity bias with respect to salinity profiles is nearly zero. Large fresh anomalies are found in tropical areas such as the western Atlantic and Pacific oceans. This surface fresh anomaly persists during the whole period covered by the reanalysis. Saltier surface waters are also found in the Arctic Ocean compared to the Levitus climatology. A general salty bias (less than 0.1 psu) is found in the [50 m-200 m] layer. Both biases and RMSD against all the in-situ observations drastically decrease with time in accordance with the increasing observations network density.

Positive trends of SSS are seen over most parts of the global ocean. Yet, local negative trends are found in the Arctic Ocean and in the Indonesian Through-flow. This overall weak (+0.002 per year) positive trend is reduced compared to the GLORYS2V4 reanalysis and mitigated by a negative trend the first three years of the reanalysis.

Along the equator, salinity profiles are highly consistent with observations with RMSD generally smaller than 0.2 psu in the water column, apart at the surface where the RMSD is higher and can intermittently reach 0.3 psu in the Atlantic Ocean. Correlations with equatorial moorings also decrease with depth with however a generally weaker correlation at the surface compared to sub-surface scores.

The global salt content shows a weak positive trend with a somehow stabilisation during the last decade. Large interannual variability is found prior the full deployment of the Argo buoys.

### **I.2.3 *Ocean currents***

GLORYS12V1 reanalysis reproduces well the main ocean currents. Mean Kinetic Energy (MKE) at 1000 m is higher than that obtained with the ANDRO Argo drift data base all along the boundary currents and the ACC. This possible overestimation of deep currents is under investigation.

The upper layers equatorial vertical dynamics structures are in good accordance with the moorings observations. The easterly surface current is however stronger in the western Pacific and the core of the Equatorial Under Current (EUC) is weaker. RMSD are generally smaller than 0.25 m.s<sup>-1</sup> in the water column with a maximum in the lower part of the EUC. Correlations with equatorial moorings also generally decrease with depth.

### **I.2.4 *Sea level***

GLORYS12V1 reanalysis is very close to altimetric observations and has a good ability to describe the sea level variability. Regional trends are particularly well reproduced. With 2.66 mm/year, the globally averaged sea level trend is however slightly underestimated compared to the Aviso SLA CCI observed estimates, e.g. 3.27 mm/year. At high northern latitudes, regions not well observed by altimetry, strong sea level trends are depicted in GLORYS12V1. The globally averaged RMSD of the analysed sea level is about 5.5 cm and the forecast sea level is 0.5 cm higher. A global and constant 0.07 cm bias is present during the 2005-2016 time period.

### **I.2.5 *Transports***

Compared to Lumpkins and Speer (2007) estimates, GLORYS12V1 generally overestimates the mean volume transport in all basins and particularly all along the ACC current (by up to 30 Sv). However, ACC volume transports at Drake passage simulated by GLORYS12V1 and GLORYS2V4 are in better accordance with latest estimations from Donohue et al. (2016) and Colin de Verdière and Ollitrault

(2016). Four GLORYS12V1 transports in the northern Atlantic and Pacific oceans sections are in opposite sign compared to the Lumpkins and Speer (2007) estimates; however, they remain in the Lumpkins and Speer (2007)'s error bars. estimates.

The Atlantic Meridional Overturning Circulation (AMOC) shows no significant trend throughout the reanalysis period. It is 3 Sv weaker than the RAPID data, but exhibits high correlation (0.86) to these data.

The Meridional Heat Transport generally is in the error bars of the Ganachaud & Wunsch (2000) and Trenberth & Caron (2001) estimates.

### **I.2.6 Sea Ice concentration**

Thanks to sea ice concentration assimilation, all the sea ice extent variability (seasonal cycle, interannual variability and trend) is well reproduced in GLORYS12V1. Both Arctic sea ice extent and volume show a general decrease of respectively -85400 km<sup>2</sup>/year and -46200 km<sup>3</sup>/year for the 1993-2016 period. Both hemispheres winter sea ice extent maxima also show overestimation with the assimilated CERSAT data. Although the year 2016 exhibits an unusual strong negative anomaly, the Antarctic sea ice extent still exhibits a positive trend of 56300 km<sup>2</sup>/year for the 1993-2016 period.

RMS deviations and biases with assimilated ice concentration dataset are stable all over the period. For the Arctic the maximum of the RMS difference with assimilated sea ice concentration dataset reach 0.25 in the summer and 0.12 in the winter. The results are generally the same with the independent dataset but somehow higher. Positives differences between the observations and the model during spring and summer show an excess of ice melting in GLORYS12V1. During the winter the differences are positives indicating a reduced spread of ice extent. Results are similar in Antarctic with however higher RMS differences (up to 0.4 in concentration).

## I.3 Estimated Accuracy Number

### **GLORYS12V1 1993-2016**

Estimated Accuracy Numbers are calculated using mean and RMS deviations from data assimilation statistics.

#### **. Temperature (Celsius degrees)**

<b>Level</b>	<b>Period</b>	1993-2016		1993-2005		2005-2016	
		<i>Mean</i>	<i>RMS</i>	<i>Mean</i>	<i>RMS</i>	<i>Mean</i>	<i>RMS</i>
0-100		-0.05	0.97	-0.03	1.00	-0.07	0.91
100-300		-0.02	0.85	0.01	0.93	-0.04	0.80
300-800		-0.005	0.48	0.01	0.55	-0.01	0.43
800-2000		0.006	0.20	-0.01	0.27	0.008	0.18

#### **Salinity (psu)**

<b>Level</b>	<b>Period</b>	1993-2016		1993-2005		2005-2015	
		<i>Mean</i>	<i>RMS</i>	<i>Mean</i>	<i>RMS</i>	<i>Mean</i>	<i>RMS</i>
0-100		-0.003	0.293	-0.007	0.407	-0.002	0.26
100-300		-0.007	0.165	-0.015	0.249	-0.004	0.13
300-800		-0.001	0.082	0.002	0.112	-0.001	0.07
800-2000		0.000	0.054	0.003	0.091	-0.001	0.04

#### **Sea Level (cm)**

<b>Period</b>	1993-2016		1993-2005		2005-2016	
	<i>Mean</i>	<i>RMS</i>	<i>Mean</i>	<i>RMS</i>	<i>Mean</i>	<i>RMS</i>
	0.003	5.5	0.002	5.3	0.07	5.5

#### **SST°C**

<b>Period</b>	1993-2016		1993-2005		2005-2016	
	<i>Mean</i>	<i>RMS</i>	<i>Mean</i>	<i>RMS</i>	<i>Mean</i>	<i>RMS</i>
	-0.05	0.5	-0.05	0.5	-0.05	0.5

## **II PRODUCTION SUBSYSTEM DESCRIPTION**

---

**Production Center: GLOBAL MFC**

**Production Unit:**

- GLORYS12V1: **Mercator Ocean**

### **II.1 GLORYS12V1 reanalysis (001\_030)**

Over the past years, Mercator Ocean has been regularly upgrading its global ocean physical reanalysis through improvements in the ocean model, assimilation scheme and assimilated data sets. The last upgrade concerned the eddy-permitting reanalysis GLORYS2V4 GLOBAL\_REANALYSIS\_PHY\_001\_025 ( $\frac{1}{4}^\circ$  horizontal resolution and 75 vertical levels, <http://marine.copernicus.eu/documents/QUID/CMEMS-GLO-QUID-001-025.pdf>) covering the altimetry era (1993-2016). In the framework of Copernicus Marine Environment Monitoring Service (CMEMS), we propose now an eddy-resolving physical reanalysis called GLORYS12V1 GLOBAL\_ANALYSIS\_FORECAST\_001\_030 (Lellouche et al, 2021), covering the same time period and based on the current real-time global forecasting CMEMS PSY4V3R1 system GLOBAL\_ANALYSIS\_FORECAST\_001\_024 ( $1/12^\circ$  horizontal resolution and 50 vertical levels, <http://marine.copernicus.eu/documents/QUID/CMEMS-GLO-QUID-001-024.pdf>).

The model component is the NEMO platform driven at the surface by ECMWF ERA-Interim reanalysis until end of 2018, ERA5 reanalysis after (see NB). Observations are assimilated by means of a reduced-order Kalman filter with a 3D multivariate modal decomposition of the background error. It includes an adaptive-error estimate and a localization algorithm. Along track altimeter data (Sea Level Anomaly – SLA), satellite Sea Surface Temperature (SST), Sea Ice Concentration and in-situ temperature and salinity (T/S) vertical profiles are jointly assimilated. Moreover, a 3D-VAR scheme provides a correction for the slowly-evolving large-scale biases in temperature and salinity.

Compared to PSY4V3R1 (see Lellouche et al, 2018), GLORYS12V1 reanalysis uses the reprocessed atmospheric forcing coming from the global atmospheric reanalysis ERA-Interim and benefits from a few changes in the system settings about observation errors.

Compared to GLORYS2V4, GLORYS12V1 reanalysis benefits from the main following updates: initial T/S conditions derived from EN4.2.0 data base, global steric effect added to the model sea level, new Glacial Isostatic Adjustment correction, new seasonal observation error for assimilation of in-situ T/S vertical profiles, adaptive tuning of observational SLA and SST errors, additional Quality Control on the assimilated T/S vertical profiles based on dynamical height criteria, assimilation in the deep ocean (below 2000 m) of climatological T/S vertical profiles using a non-Gaussian error at depth. New and improved reprocessed in situ and satellite data sets have also been used.

In order to provide a synthetic view of the consistency between the PSY4V3R1 real time  $1/12^\circ$  analyses GLOBAL\_ANALYSIS\_FORECAST\_001\_024 and the GLORYS12V1 reanalysis GLOBAL\_ANALYSIS\_FORECAST\_001\_030, GLORYS12V1's configuration setup was compared with that of PSY4V3R1 and GLORYS2V4 and this comparison was summarized in Tables 1 and 2 of this document. The reader will find complementary references and initial description of the system set up in <http://marine.copernicus.eu/documents/QUID/CMEMS-GLO-QUID-001-024.pdf> and <http://marine.copernicus.eu/documents/QUID/CMEMS-GLO-QUID-001-025.pdf>.

**NB:** A change in GLORYS12V1 reanalysis occurs at the beginning of the year 2019. The atmospheric forcing flux used to force GLORYS12V1 has been switched from ERAinterim to ERA5.

**Quality Information Document  
For products  
GLOBAL\_REANALYSIS\_PHY\_001\_030**

Ref :CMEMS-GLO-QUID-001-030  
Date : September 2021  
Issue : 1.5

Before applying this modification, sensitivity tests have been performed over the year 2017 using GLORYS2V4 (Mercator Ocean global  $\frac{1}{4}$  reanalysis, members of GREP product; see global-reanalysis-phy-001-031 CMEMS product). No major change was observed in the comparison to observed data for oceanic variables. The only visible change is a reduction, during austral summer, in the ice volume and extent in Southern Ocean with the use of ERA5.

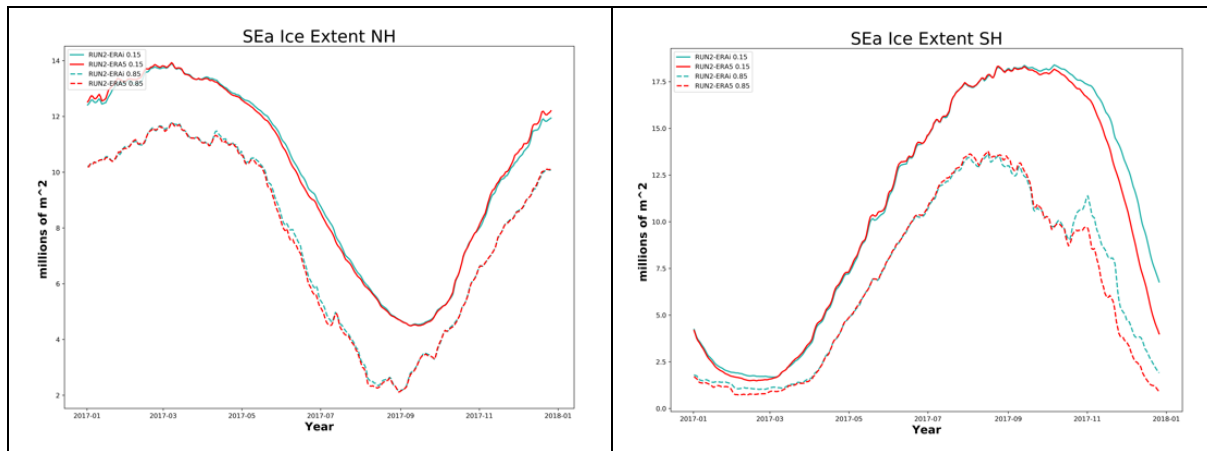


*Figure 1 Evolution of Sea Ice Extent for northern (left) and southern hemisphere (right) for the simulation forced with ERAinterim (blue) and ERA5 (red). Both criteria at 85% (solid line) and 15% (dashed line) are plotted.*

**Quality Information Document**  
**For products**  
**GLOBAL\_REANALYSIS\_PHY\_001\_030**

Ref :CMEMS-GLO-QUID-001-030  
Date : September 2021  
Issue : 1.5

PSY4V3R1	GLORYS2V4	GLORYS12V1
GLOBAL_ANALYSIS_FORECAST_001_024	GLOBAL_REANALYSIS_PHY_001_025	GLOBAL_REANALYSIS_PHY_001_030
50 z-levels	75 z-levels	= PSY4V3R1
ECMWF operational atmospheric analyses(IFS) with 3H frequency No snowfall	ECMWF atmospheric reanalysis ERAinterim (ERAi)3H/24H frequency + diurnal cycle Snowfall ER5 after January 2019	= GLORYS2V4
Large scale correction of IFS precipitations (towards PMWC)	Large scale correction of ERAi precipitations (towards GPCPV2.2 observations) and radiative fluxes (towards GEWEX SRB3.0 & 3.1 observations) ERA5 without correction after 2019.	Large scale correction of ERAi precipitations (towards PMWC observations) and radiative fluxes (towards GEWEX SRB3.0 & 3.1 observations) ERA5 without correction after 2019.
Initial Conditions (December 2006) estimated from EN4.2.0 monthly gridded fields for December 2006 using a regression technique	Initial Conditions (December 1991) estimated from EN4.0.2 monthly gridded fields for December 1991 using a regression technique	Initial Conditions (December 1991) estimated from EN4.2.0 monthly gridded fields for December 1991 using a regression technique
Surface mass Budget EMP (Evaporation – Precipitation –run off)=0 + seasonal cycle + 2.2 mm/yr (2007-present).	Surface mass Budget EMP=0 + seasonal cycle + 1.74 mm/yr (1993-2016).	Surface mass Budget EMP=0 + seasonal cycle + 1.31 mm/yr (1993-2001) + 2.2 mm/yr (2002-2016).
Global steric effect diagnosed from T and S and added to SSH	None	= PSY4V3R1
Turbulent Kinetic Energy (TKE) mixing scheme with mixing length set to 30 m	TKE with mixing length set to 10 m	=GLORYS2V4
Restoring to WOA13 2005-2013 decadal climatological temperature and salinity at Gibraltar and Bab-El-Mandeb straits	Restoring to EN4.0.2 decadal climatology at Gibraltar and Bab-El-Mandeb straits	Restoring to EN4.2.0 decadal climatology at Gibraltar and Bab-El-Mandeb straits
Climatological Runoff Dai et al (2009) + freshwater fluxes from icebergs for Greenland and Antarctica	= PSY4V3R1	= PSY4V3R1
Solar penetration 3 bands (RGB)	Solar penetration 2 Bands	= GLORYS2V4
Relative wind with 50% ocean currents in momentum flux	= PSY4V3R1	= PSY4V3R1
Outputs: HF (1h) + daily mean + coarsened files at %° for biogeochemistry	Outputs : daily mean	= PSY4V3R1

*Table 1: Model configuration of GLORYS12V1, compared with that of PSY4V3R1 and GLORYS2V4.*

**Quality Information Document**  
**For products**  
**GLOBAL\_REANALYSIS\_PHY\_001\_030**

Ref :CMEMS-GLO-QUID-001-030  
Date : September 2021  
Issue : 1.5

<b>PSY4V3R1</b> GLOBAL_ANALYSIS_FORECAST_001_024	<b>G2V4</b> GLOBAL_REANALYSIS_PHY_001_025	<b>G12V1</b> GLOBAL_REANALYSIS_PHY_001_030
Assimilation of CORA4.1 in situ dataset until 2003 (early version of INSITU_GLO_TS REP_OBSERVATIONS_013_001_b). From 2014 to present, the near-real time CMEMS product INSITU_GLO_NRT_OBSERVATIONS_013_030 is assimilated.	= PSY4V3R1	Assimilation of CORA4.1 until 2003. From 2014 to 2015, CORA5.0 product is assimilated. For 2016, CORA5.1 product is assimilated.
Assimilation of sea ice concentration from OSISAF  SEAICE_GLO_SEAICE_L4 REP_OBSERVATION_S_011_009	Assimilation of sea ice concentration from CERSAT	= GLORYS2V4 + OSISAF only as verification
Assimilation of SST OSTIA  SST_GLO_SST_L4_NRT_OBSERVATIONS_010_001	Assimilation of NOAA SST analyses at $\frac{1}{4}^{\circ}$ (AVHRR)	= GLORYS2V4
Hybrid Mean Dynamic Topography (MDT) based on CNES-CLS13 + new glacial isostatic adjustment file	Hybrid MDT based on CNES-CLS13	= PSY4V3R1
Error covariance (ocean + sea ice state anomalies) from twin simulation of PSY4V3R1 (only corrected from large scale T and S biases) + spatial filtering	Error covariance (ocean + sea ice state anomalies) from a consistent free global simulation	= PSY4V3R1
3D T/S in-situ observations errors from GLORYS2V3	3D T/S in-situ observations errors from GLORYS2V2	3D T/S in-situ seasonal observations errors from PSY4V3R1
Adaptive tuning for SST and SLA observation errors	Fixed errors from 2 cm to 5.5 cm (instrument dependency) for SLA and 0.6°C for SST + representativity error map	Adaptive tuning for SST and SLA observation errors + specification of a 2D minimum error map
2 layers of quality control are applied (QC1 & QC2)	Only QC1 is applied	= PSY4V3R1

**Quality Information Document  
For products  
GLOBAL\_REANALYSIS\_PHY\_001\_030**

Ref :CMEMS-GLO-QUID-001-030  
Date : September 2021  
Issue : 1.5

PSY4V3R1	G2V4	G12V1
Assimilation of WOA13 profiles below 2000 m with non-Gaussian observation error distribution	Restoring to Gouretski et al (2004) climatology below 2000 m and poleward 60°S	Assimilation of EN4.2.0 profiles below 2000 m with non-Gaussian observation error distribution
3D-VAR Bias Correction on a 3-month window	= PSY4V3R1	3D-VAR Bias Correction on a 3-month window until the end of 2003 and 1-month window beyond
Total SSH increment from the analysis	SSH increment split in HBAR from the analysis and HDYN from 3D T/S increments	= PSY4V3R1
Global mean of total SSH increment = 0	Global mean of steric SSH increment = 0	= PSY4V3R1
TSUV equatorial pseudo-observations in [150 m-3000 m] layer	= PSY4V3R1	= PSY4V3R1
Due to adaptive tuning of observation errors, no amplification of SLA and SST observation error with observations density	Amplification of SLA and SST observation error with observations density	= PSY4V3R1
SST observation: 1 out of every 4 points on the $\frac{1}{4}^{\circ}$ ORCA grid	SST observation: 1 out of every 2 points on the $\frac{1}{4}^{\circ}$ ORCA grid	= PSY4V3R1

*Table 2: Data assimilation configuration of GLORYS12V1, compared with that of PSY4V3R1 and GLORYS2V4.*

### **III VALIDATION FRAMEWORK**

---

The validation methodology defined and used to validate the global ocean reanalysis products is described in Drevillon et al (2018) and consists in a series of diagnostics defined in common by all global ocean reanalysis / reference forced simulation producers.

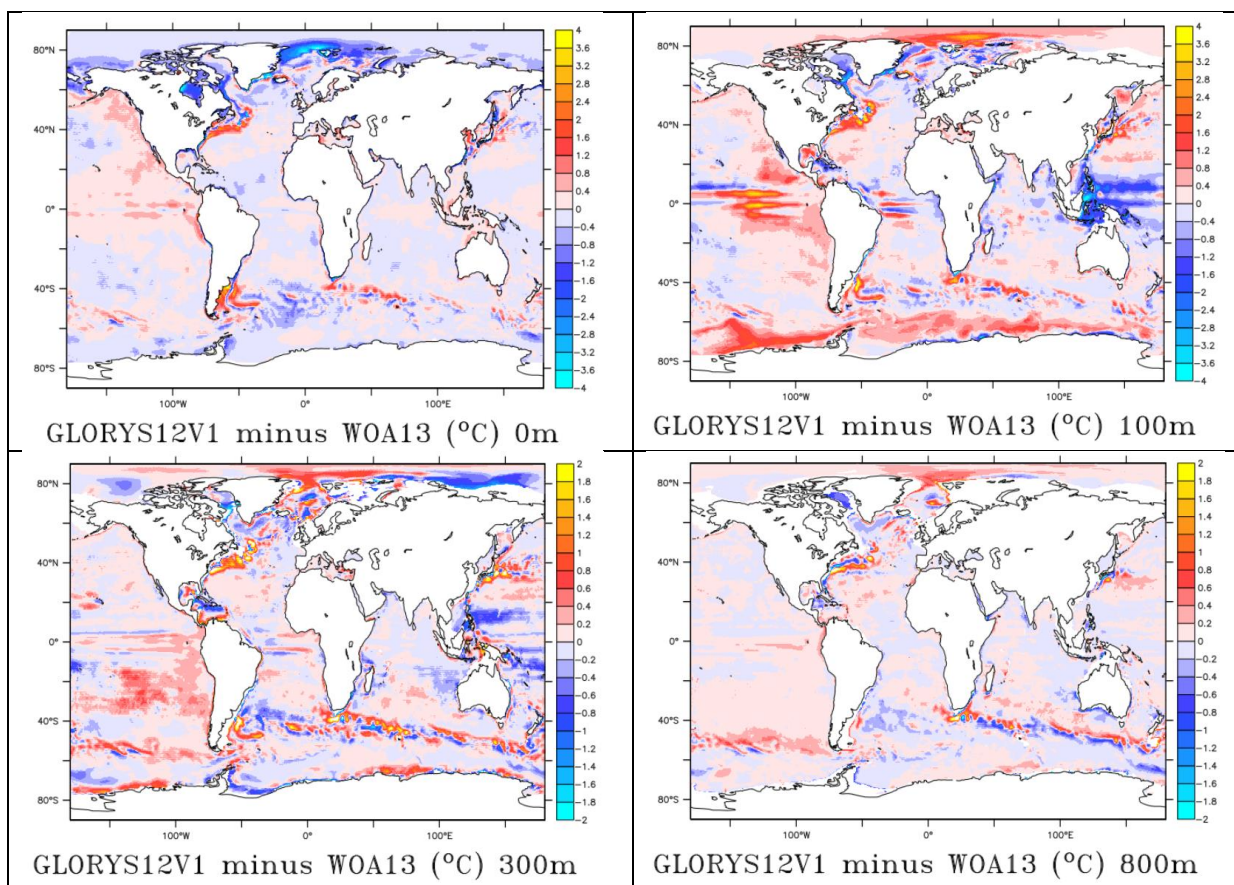
The reference validation period is 1<sup>st</sup> January 1993 – 31 December 2016. The times series are based on monthly fields except for the innovation diagnostics (see T-DA\_INNO\_STAT, S-DA\_INNO\_STAT, SL-DA-INNO\_STAT, SI-CONC-DA-INNO\_STAT sections).

## IV VALIDATION RESULTS OF GLORYS12V1

### IV.1 Temperature

#### IV.1.1 T-CLASS1-T3D-MEAN

As shown by Fig. 1.1 GLORYS12V1 reanalysis has weak regional biases (less than 0.4 °C) in temperature with respect to the World Ocean Atlas 2013 climatology. The largest biases occur in the [50 m-100 m] layer and in the northern Atlantic and Southern oceans.



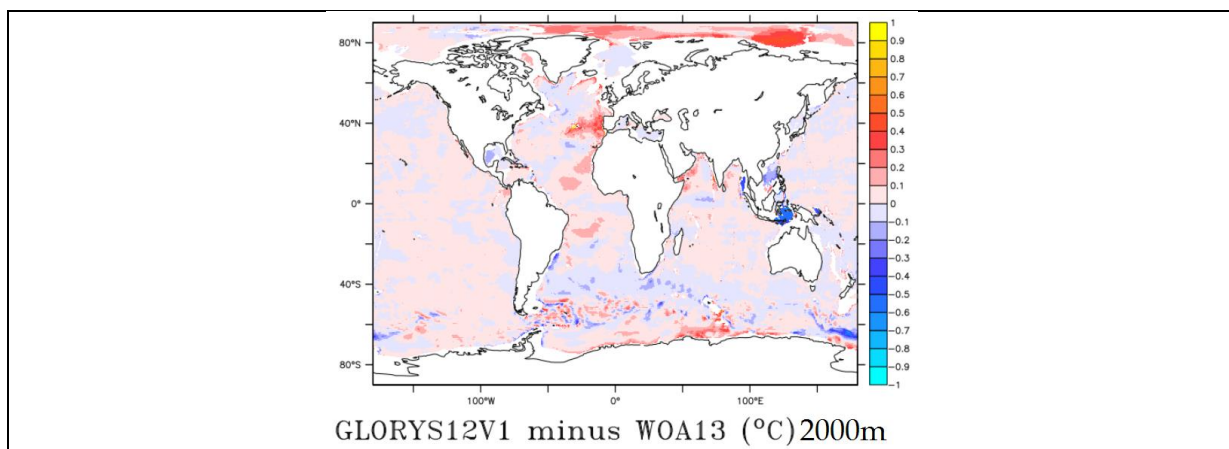


Fig. 1.1: Differences of temperature (in °C) between GLORYS12V1, and the World Ocean Atlas 2013 climatology (WOA13) near 0 m, 100 m, 300 m, 800 m and 2000 m depth, respectively. For this comparison, model data have been averaged over the period 1993 – 2016 (note colour scale changes).

#### IV.1.2 T-CLASS1-SST-MEAN

The global mean sea surface temperature (SST hereafter) is close to the observations with a weak (warm) misfit of less than 0.1°C all along the reanalysis (Fig. 1.2). The global positive SST linear trend (Fig. 1.3) is highly consistent with AVHRR data.

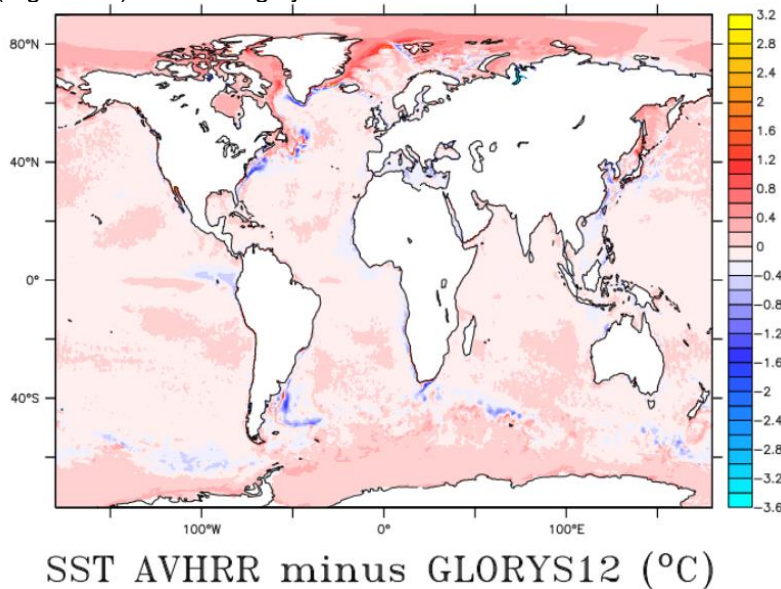


Fig. 1.2: Mean 1993-2016 difference in sea surface temperature (°C) between GLORYS12V1 and the AVHRR SST data.

#### IV.1.3 **T-CLASS1-SST-TREND**

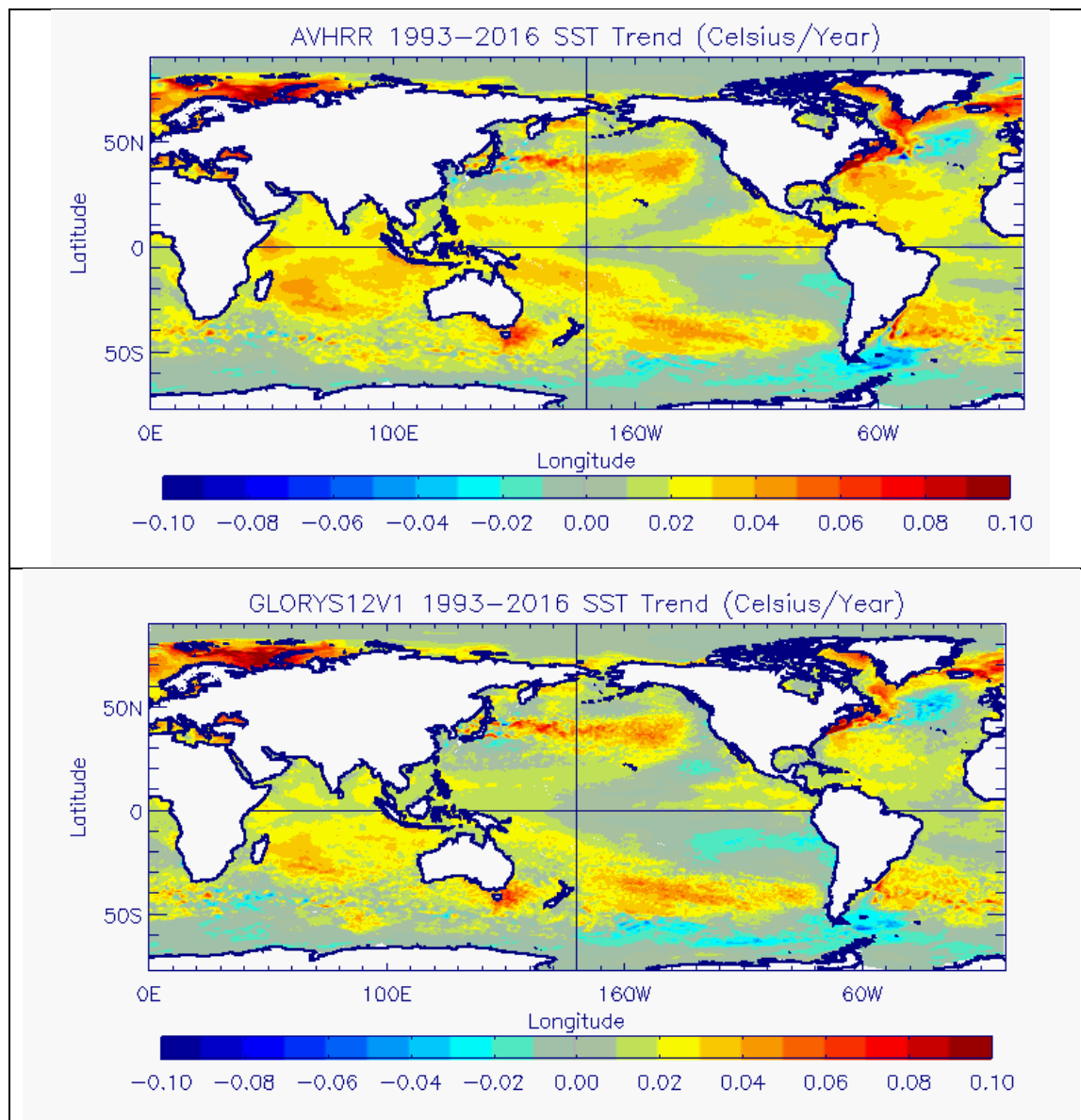


Fig. 1.3: Linear 1993-2016 SST trend of AVHRR data (upper panel) and GLORYS12V1 (bottom panel).

#### IV.1.4 T-CLASS2-MOORINGS

Along the equator, temperature profiles are very consistent with observations (Fig 1.4) with RMSD (Root mean square errors) generally smaller than 0.4°C in the water column, apart from the [50 m-200 m] layers where the RMSD can intermittently reaches 1.2°C in the Indian Ocean. Correlations with equatorial moorings also decrease with depth.

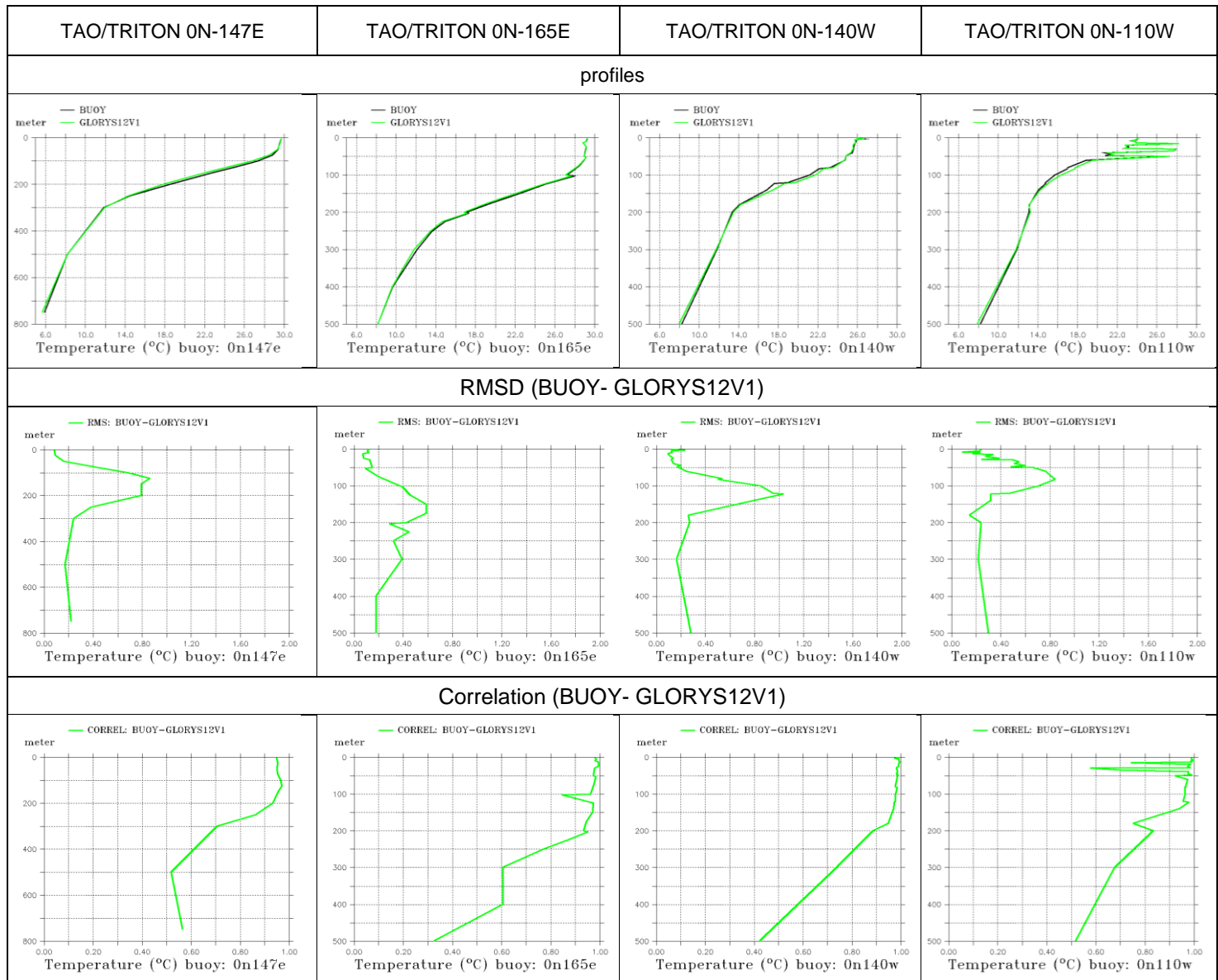


Fig. 1.4: Mean equatorial temperature profile (top), RMSD (middle), correlation (bottom) estimated over the period 1993 – 2015: observations (black) and GLORYS12V1 (green). Mooring observations are coming from TAO/TRITON: 0N-140W, 0N-110W, 0N-165E, 0N-147E, PIRATA: 0N-23W, 0N-0E and RAMA: 0N-90E (continues in next page).

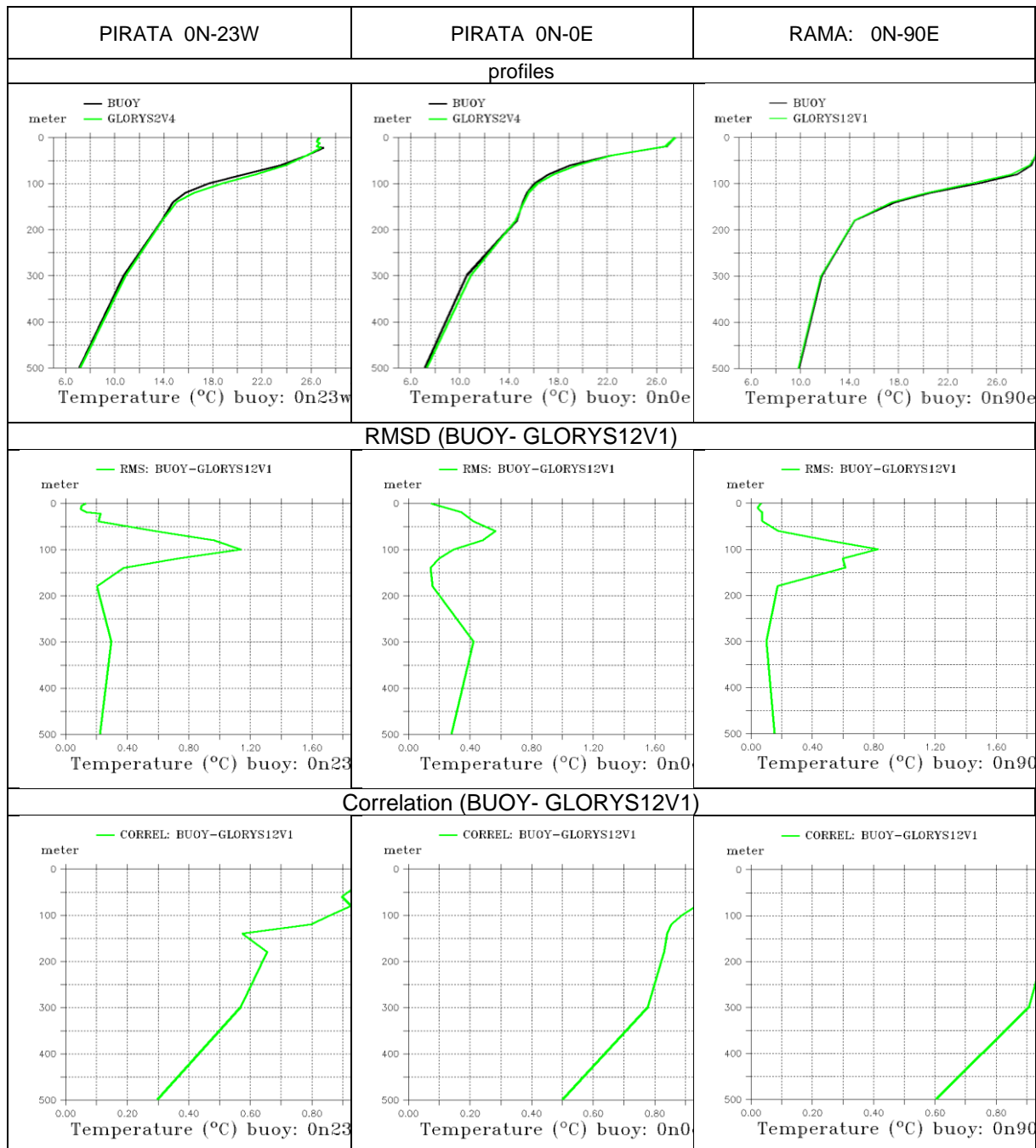


Fig. 1.4: (continued) Mean equatorial temperature profile (top), RMSD (middle), correlation (bottom) estimated over the period 1993 – 2015: observations (black) and GLORYS12V1 (green). Moorings observations are coming from TAO/TRITON: 0N-140W, 0N-110W, 0N-165E, 0N-147E, PIRATA: 0N-23W, 0N-0E and RAMA: 0N-90E.

#### IV.1.5 T-CLASS3-SST\_QNET\_MEAN

The global mean surface net heat flux is weakly negative over the period (- 0.7 W.m<sup>2</sup>) as can be seen in Fig 1.5. The globally averaged linear trend for net surface heat flux is -0.35 W.M<sup>2</sup>/year, while the globally average linear SST trend is close to observations (it is +0.013 °C/year for AVHRR and +0.018 for GLORYS12V1).

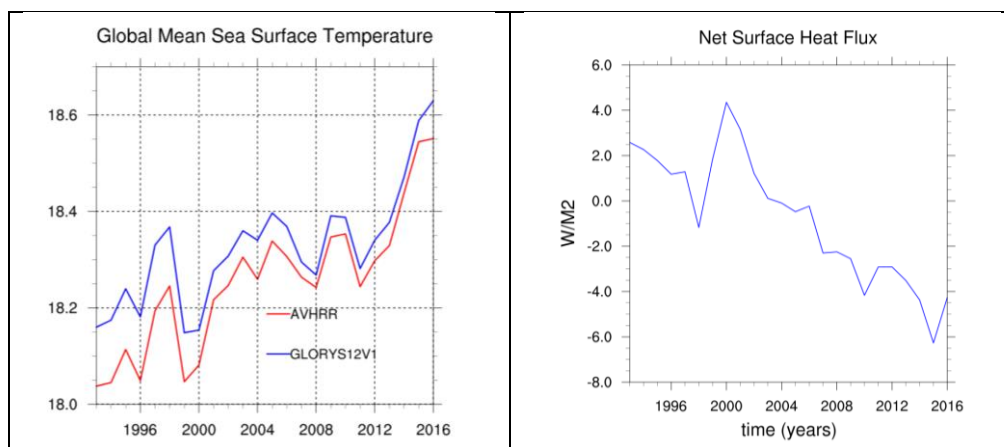


Fig. 1.5: Global annual spatial average of SST (left, °C) and surface net heat flux (right, W.m<sup>-2</sup>) for the 1993-2016 period. Assimilated SST AVHRR observations are in black (left panel only) and GLORYS12V1 in blue

#### IV.1.6 T-CLASS3-HC\_LAYER

The heat content (fig 1.6) constantly increases with time until 2011. Since 2011, the heat content may have stabilised. Only the deeper layers (below 2000 m depth) show a constant cooling.

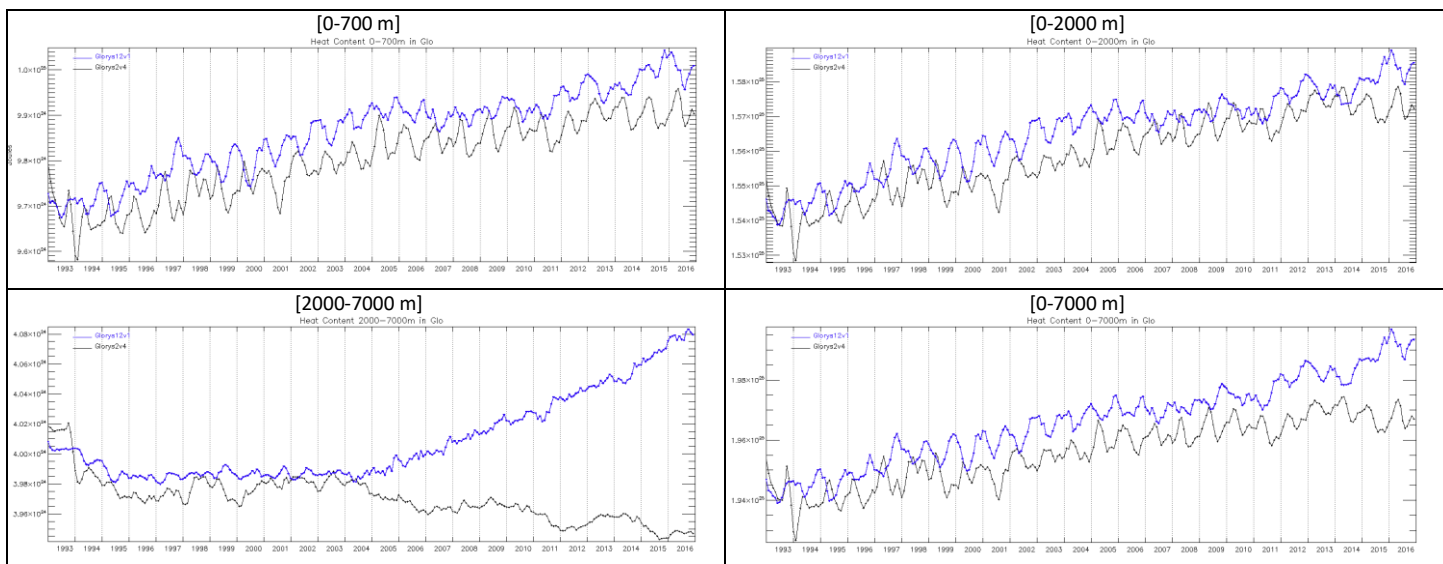


Fig. 1.6: Time evolution (1992-2016) of global average of temperature in different layers [0-700 m], [0-2000 m], [2000 m-bottom] and [0-bottom] layers for GLORYS2V4 (black) and GLORYS12V1 (blue).

## IV.1.7 T-CLASS4-LAYER

For this validation we use the in-situ dataset coming from Copernicus Marine Service (INSITU\_GLO\_TS\_OA\_NRT\_OBSERVATIONS\_013\_002\_A). A lot of data present in this product have not been assimilated in the reanalysis because a daily subsampling is performed prior to data assimilation. The following plots are showing statistics for different layers for the variables temperature and salinity.

### IV.1.7.1 Timeseries

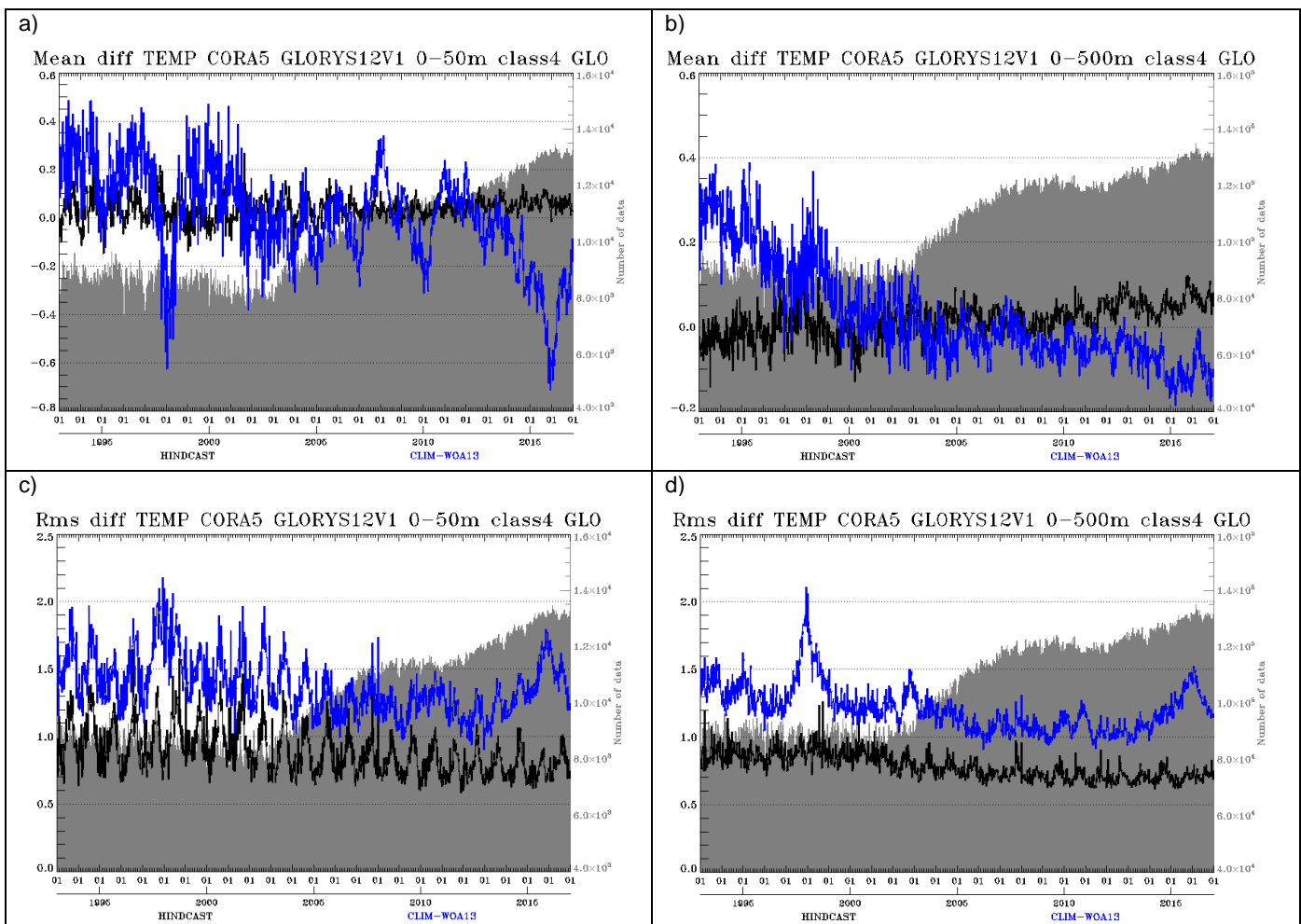
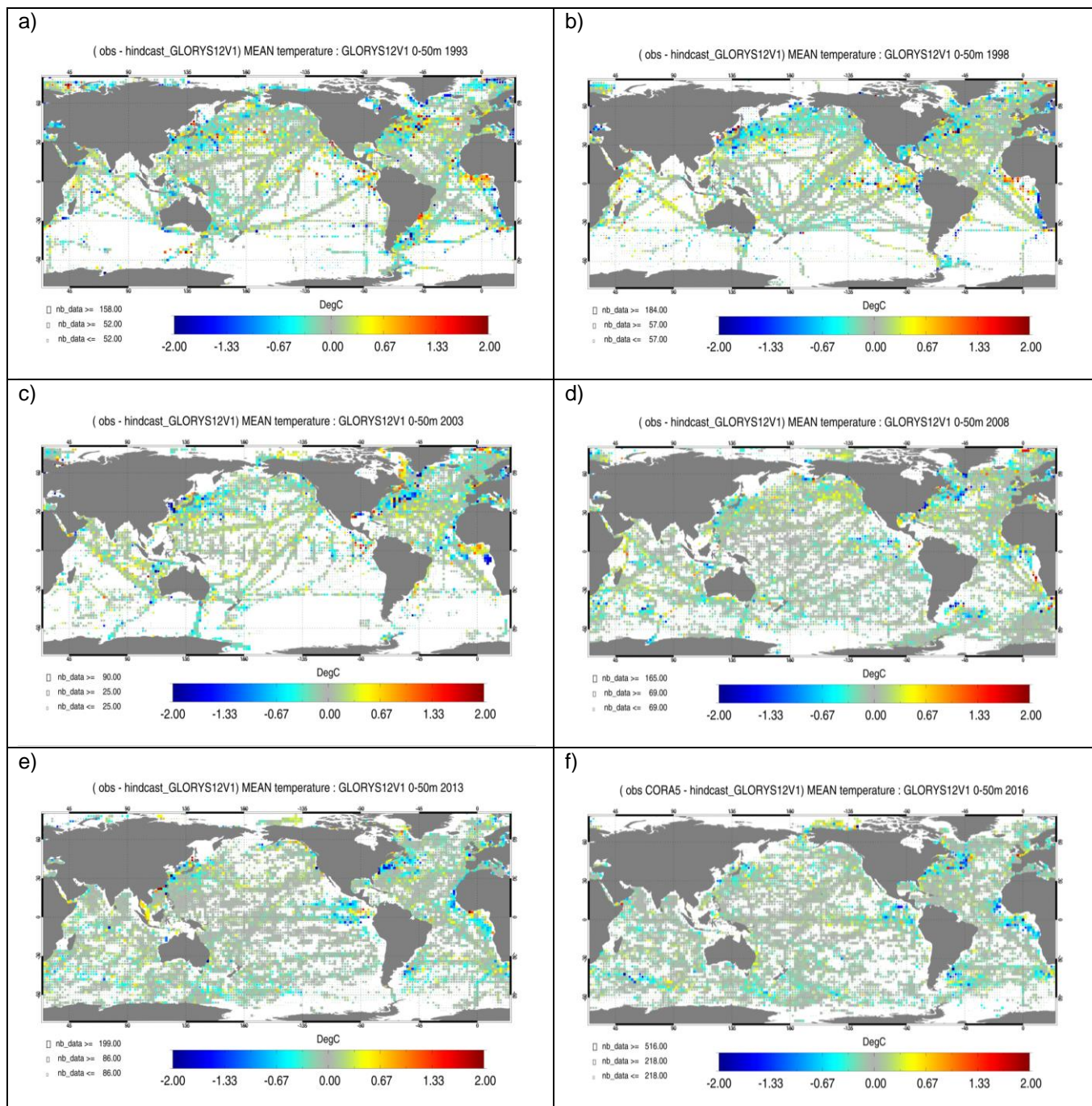


Figure 1.7.1 Timeseries (1993-2017) of mean (a, b) and RMS difference (c, d) between model Temperature and observations in black and Temperature from climatology WOA13 and observations in blue, in the 0-50 m depth layer (a, c) and 0-500 m depth layer (b, d).

When we look at the global average timeseries in Fig 1.7.1, the RMSD look very noisy until the Argo program in the 2000's. Before this date the number of in-situ data is low and the distribution is very poor (see also Fig 1.7.2) so the global statistics are not fully representative of the global ocean for the beginning of the reanalysis. After this period we see a sharp increase in the number of data and stability in the scores for the two layers displayed in Figure : 0-50 m and 0-500 m. When we look at the differences between the model and the observations we see that the reanalysis is very stable from the

2000's up to 2016. For the temperature we have a small warm bias (up to 0.1°C) in the 0-500 m layer (located between 100 and 200 m). For that variable the reanalysis beat the climatology for the bias and the RMS with lower RMS differences in the 0-500 m layer depth.

#### IV.1.7.2 2D Maps



*Figure 1.7.2: Average difference Observation-Model of temperature for the years 1993 a), 1998 b), 2003 c), 2008 d), 2013 e), 2016 f) between the daily average analysis and all available T/S observations from the Cora5.0 product. The Mercator reanalysis products are taken at the time and location of the*

*observations. Averages are performed in the 0-50 m layer and the size of the pixel in proportional to the number of observations use the compute the difference in 2°x2°boxes.*

Looking at the 2D maps (fig 1.7.2), the warm bias diagnosed in the timeseries Fig 1.7.1 appears clearly in the East of tropics, in the Gulf Stream region, the Yellow Sea, along the west coast in Africa and slightly in the Antarctic counter current region.

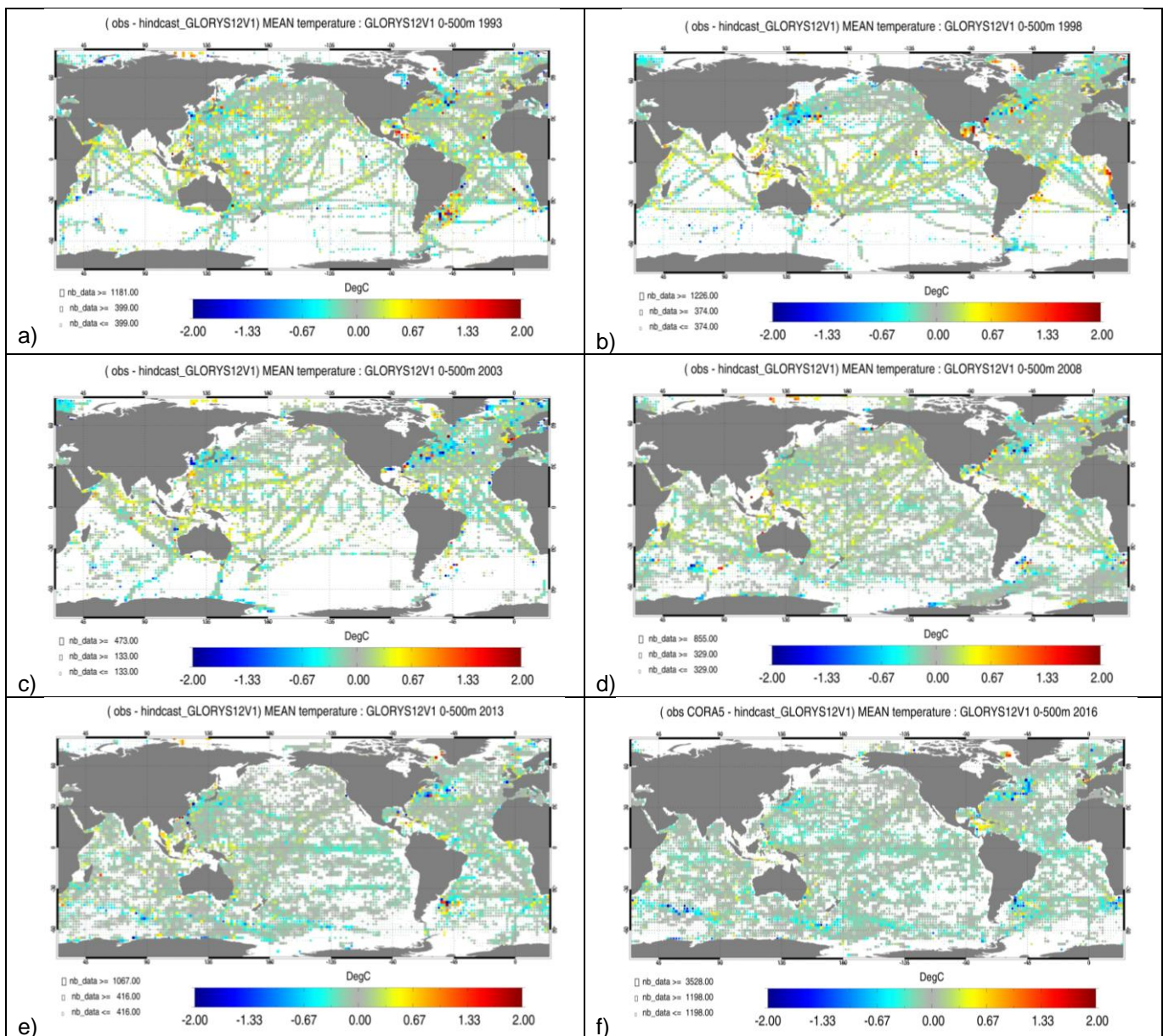


*Figure 1.7.3: Average difference Observation-Model of temperature for the years 1993 a), 1998 b), 2003 c), 2008 d), 2013 e), 2016 f) between the daily average analysis and all available T/S observations from the Cora5.0 product. The Mercator reanalysis products are taken at the time and location of the observations. Averages are performed in the 0-500 m layer and the size of the pixel in proportional to the number of observations use the compute the difference in 2°x2°boxes.*

For the 0-500 m, the warm appears in the Pacific, the Gulf Stream region and in the tropics (fig 1.7.3). The evolution of the maps highlights the increase of the in-situ network. In the last year of the reanalysis

the distribution of the in-situ data is quite uniform all over the world except in polar regions. This warm bias is probably due to some issues in the mean sea surface height in the south of the Pacific Ocean.

#### IV.1.8 T-DA-INNO-STAT

The Temperature innovations in Fig 1.8 reflect the results obtained with CLASS4 in section IV.1.7. A warm bias is diagnosed at the surface ( $0.1^{\circ}\text{C}$  on average) and slight warming trend can be seen on the water column (observation – model differences) in fig 1.8. A focus on recent years shows that despite the fact that the average innovation stays stable in time, the seasonal bias linked to restratification issues in the model tends to increase at the end of the period.

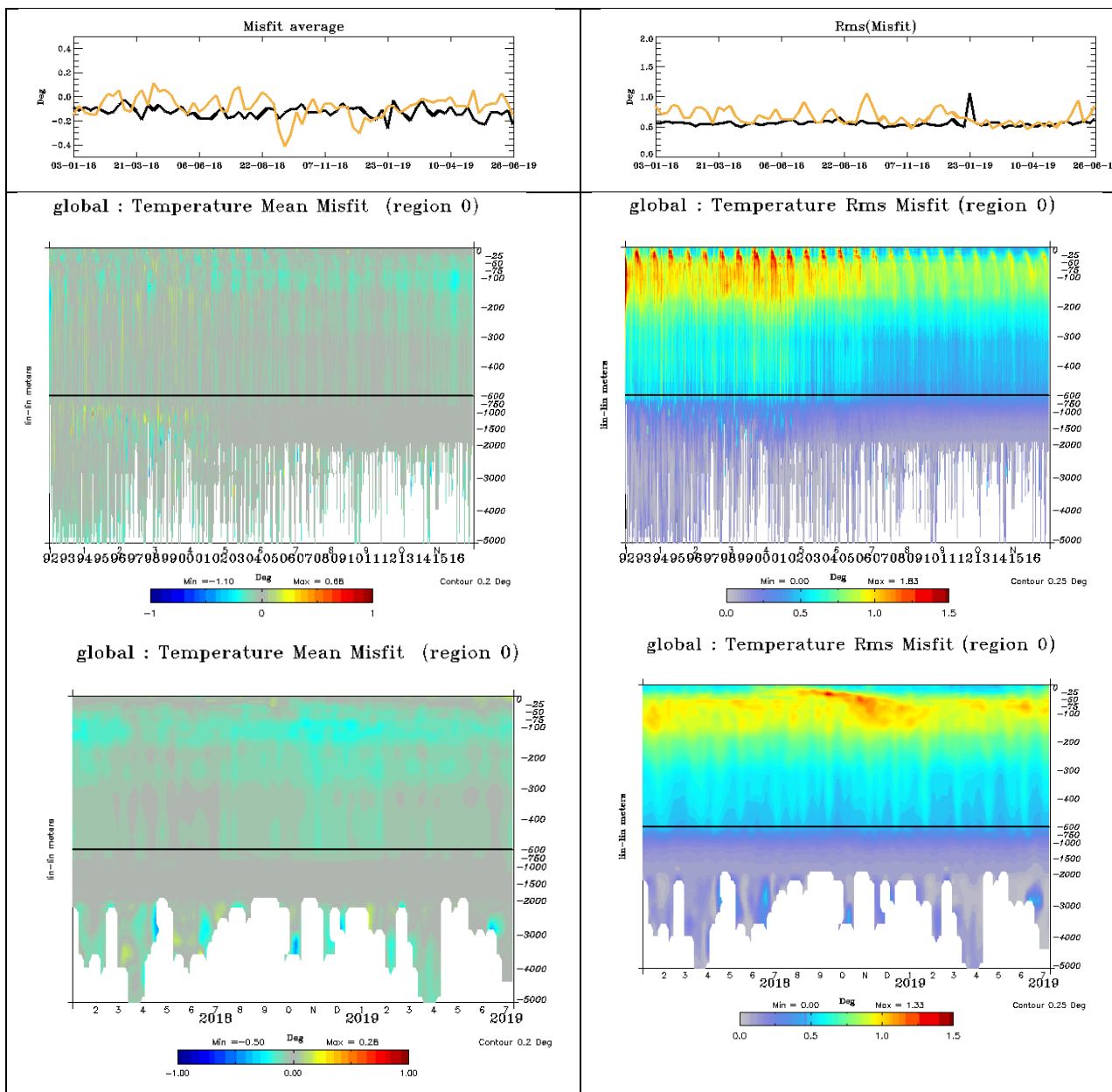


Fig. 1.8: Time evolution of the domain averaged innovation in terms of bias (left) and RMSD (right): SST (top) and CORA 4.1 in-situ temperature profiles (bottom). Top: AVHRR SST data (black), CORA4.1 SST data (orange) ( $^{\circ}\text{C}$ ). Covered time period: 1993 – 2016 and zoom on the more recent period Jan 2018–July 2019.

**Quality Information Document  
For products  
GLOBAL\_REANALYSIS\_PHY\_001\_030**

Ref :CMEMS-GLO-QUID-001-030

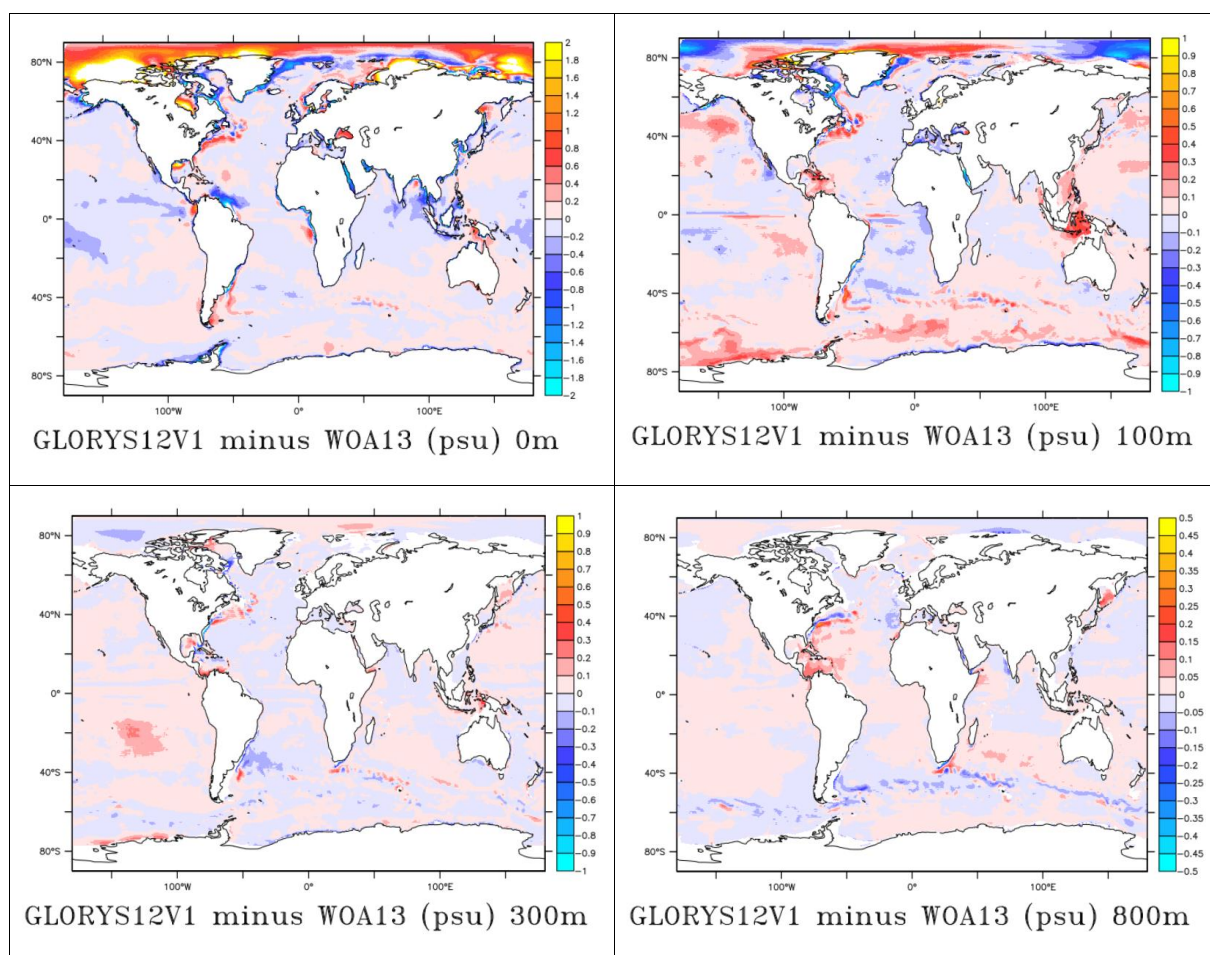
Date : September 2021

Issue : 1.5

## IV.2 Salinity

### IV.2.1 S-CLASS1-S3D\_MEAN

As seen in Fig. 2.1, the sea surface salinity (SSS hereafter) is generally fresher than the climatology with regional biases of less than 0.2 psu, except in the Arctic where larger biases appear. GLORYS is fresher than the climatology in the Amazon plume and in the Indonesian area and western tropical pacific where large precipitation events take place which may be overestimated, while at mid latitudes the model is too salty. As expected, the largest signals correspond to large variability areas (strong currents, Indonesian throughflow).



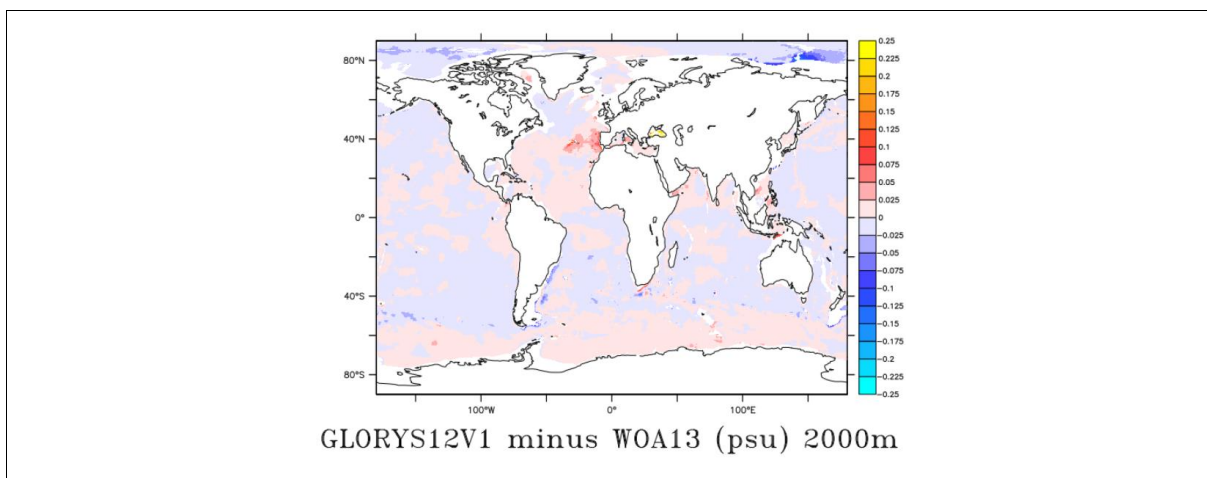


Fig. 2.1: Differences of salinity (in psu) between GLORYS12V1 and the World Ocean Atlas 2013 climatology (WOA13) near 0 m, 100 m, 300 m, 800 m and 2000 m depth. GLORYS12V1 data have been averaged over the period 1993 – 2016 (note colour scale changes).

#### IV.2.2 S-CLASS1-SSS-TREND

Positive trends of SSS are seen over most parts of the global ocean in Fig 2.2. Yet, local negative trends are found in the Arctic Ocean and in the Indonesian Through-flow. This overall weak (+0.002 per year) positive trend is reduced compared to the GLORYS2V4 reanalysis and mitigated by a negative trend the first three years of the reanalysis.

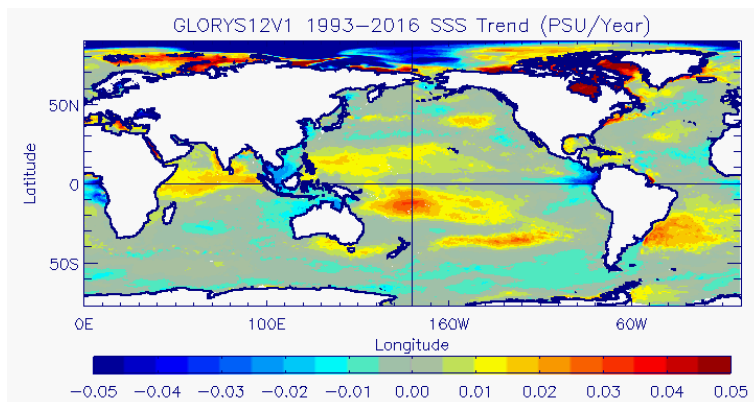


Fig. 2.2: Linear 1993-2016 SSS trend of GLORYS12V1.

#### IV.2.3 S-CLASS2-MOORINGS

Along the equator, salinity profiles (fig 2.3) are highly consistent with moorings' observations with RMSD generally smaller than 0.2 psu in the water column, apart at the surface where the RMSD is higher and can intermittently reach 0.3 psu in the Atlantic Ocean. Correlations with equatorial moorings also decrease with depth with however a generally weaker correlation at the surface compared to sub-surface scores.

**Quality Information Document**  
**For products**  
**GLOBAL\_REANALYSIS\_PHY\_001\_030**

Ref :CMEMS-GLO-QUID-001-030  
Date : September 2021  
Issue : 1.5

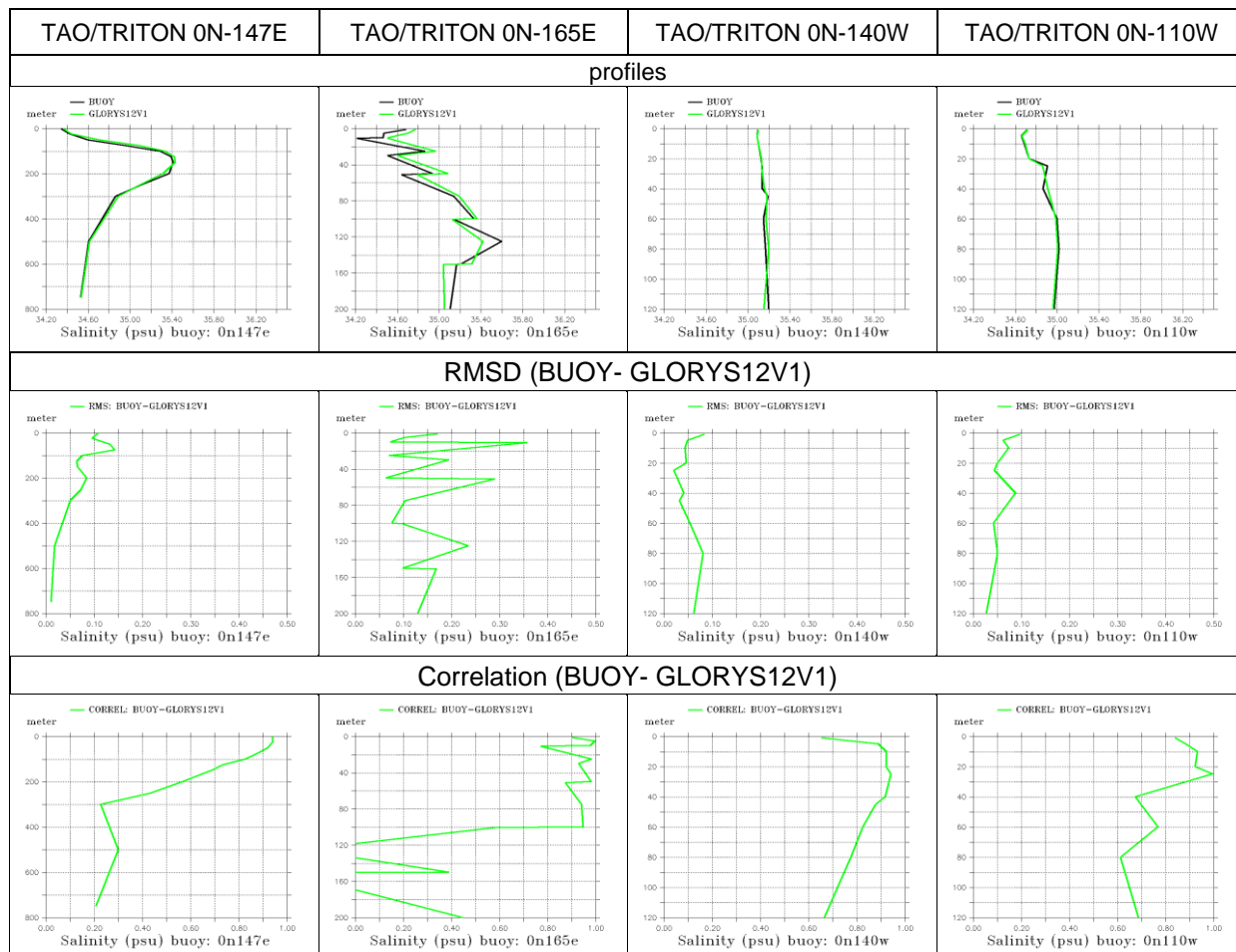


Fig. 2.3: Mean equatorial salinity profile (top), RMSD (middle) and correlation (bottom) estimated over the period 1993 – 2015: observations (TAO/TRITON: 0N-140W, 0N-110W, 0N-165E, 0N-147E, PIRATA: 0N-23W, 0N-0E and RAMA: 0N-90E) (black) and GLORYS12V1 (green) (continues in next page).

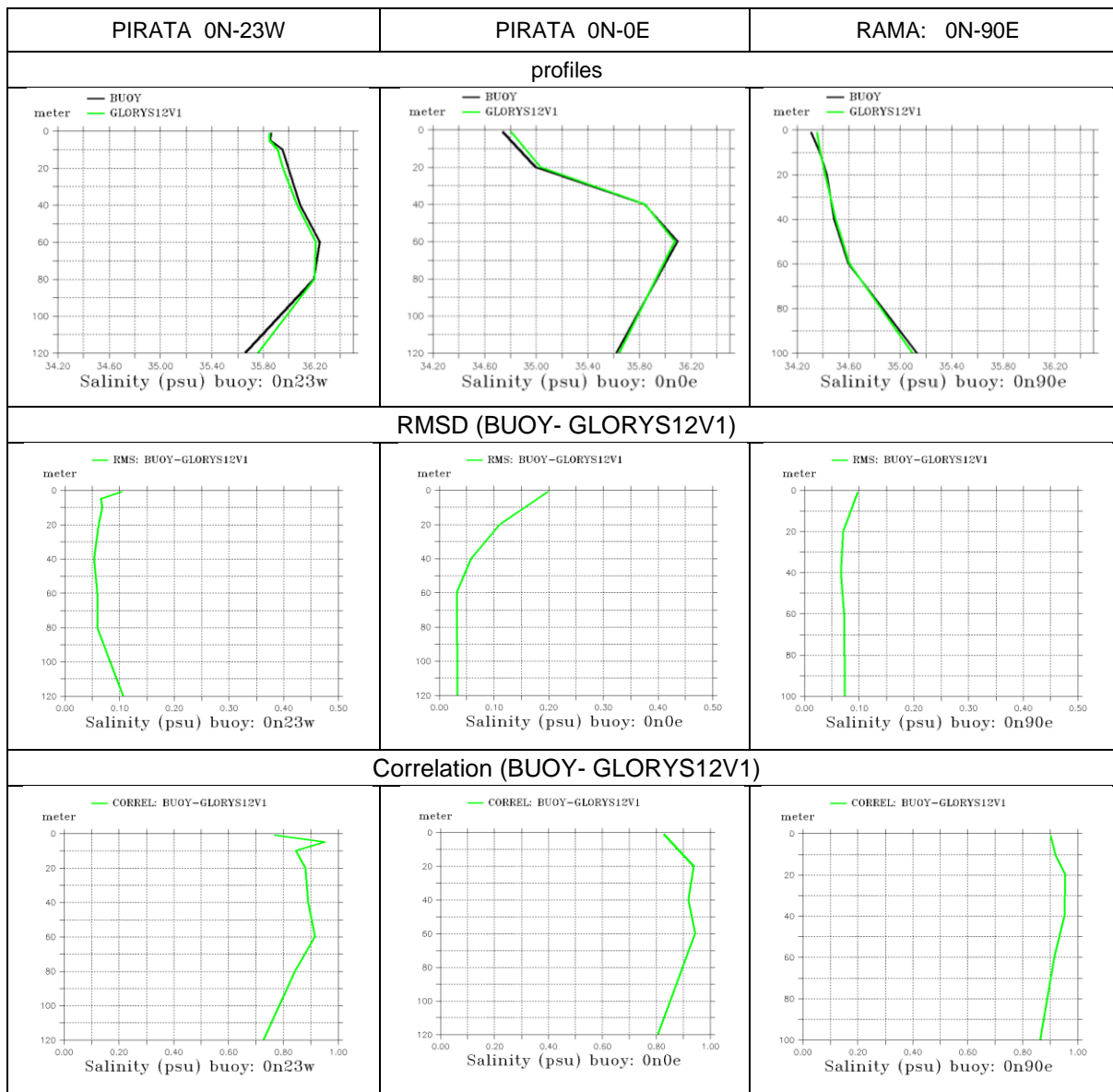


Fig. 2.3: (continued) Mean equatorial salinity profile (top), RMSD (middle) and correlation (bottom) estimated over the period 1993 – 2015: observations (TAO/TRITON: 0N-140W, 0N-110W, 0N-165E, 0N-147E, PIRATA: 0N-23W, 0N-0E and RAMA: 0N-90E) (black) and GLORYS12V1 (green).

#### IV.2.4 S-CLASS3-SSS\_SFW\_2DMEAN

As can be seen in Fig 2.4, the long term mean value of the SSS is 34.52 for GLORYS12V1 and 34.51 for GLORYS2V4 and net surface fresh water in both GLORYS12V1 and GLORYS2V4 is -0.005 mm/day.

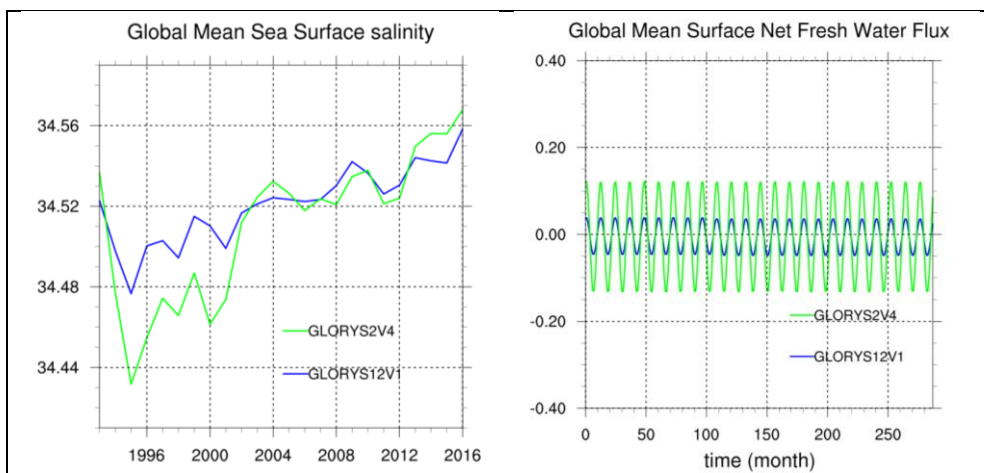


Fig. 2.4: Global spatial average of annual means SSS from (left,) and monthly means surface net fresh water heat flux (right, mm.day<sup>-1</sup>) over the period 1993 – 2016 from GLORYS12V1 (blue) and GLORYS2V4 (green)..

#### IV.2.5 S-CLASS3-SC\_LAYER

The global salt content (fig 2.5) shows a weak positive trend with a somehow stabilisation during the last decade. Large interannual variability is found prior the full deployment of the Argo buoys.

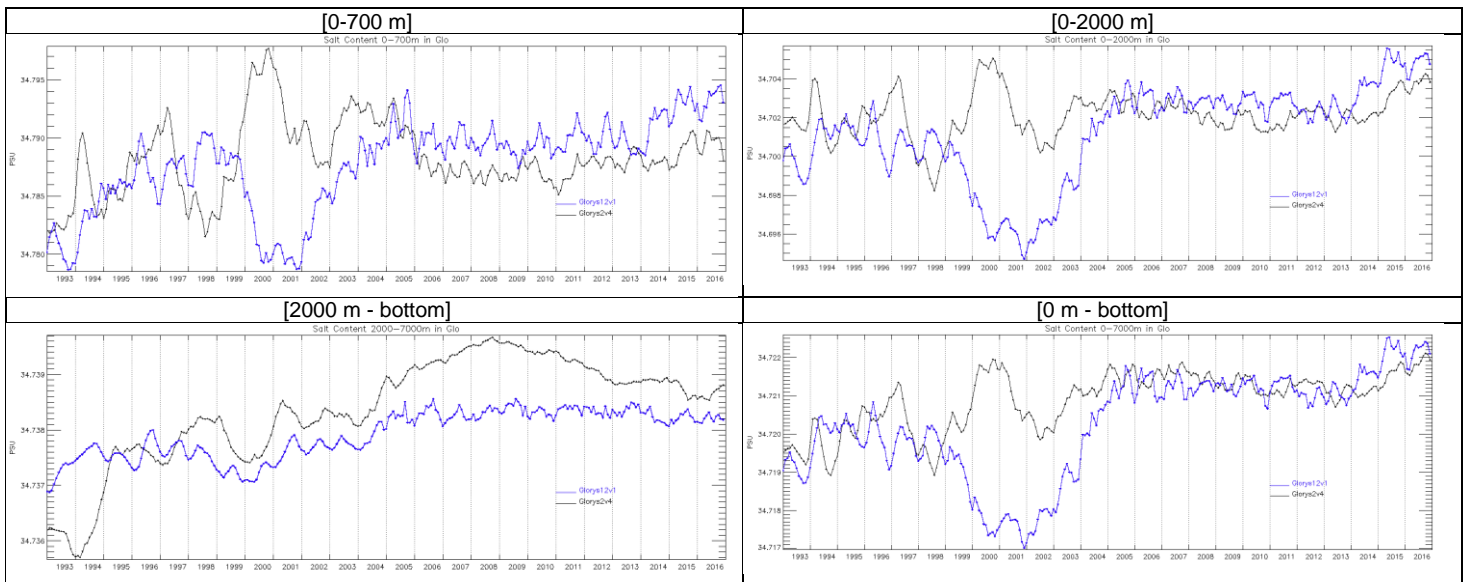


Fig. 2.5: Time evolution of global spatial average of salinity (psu) in [0-700 m], [0-2000 m], [2000 m-bottom] and [0-bottom] layers for GLORYS2V4 (black) and GLORYS12V1 (green).

## IV.2.6 S-CLASS4-LAYER

For this validation we use the same product than in IV.1.7

### IV.2.6.1 Timeseries

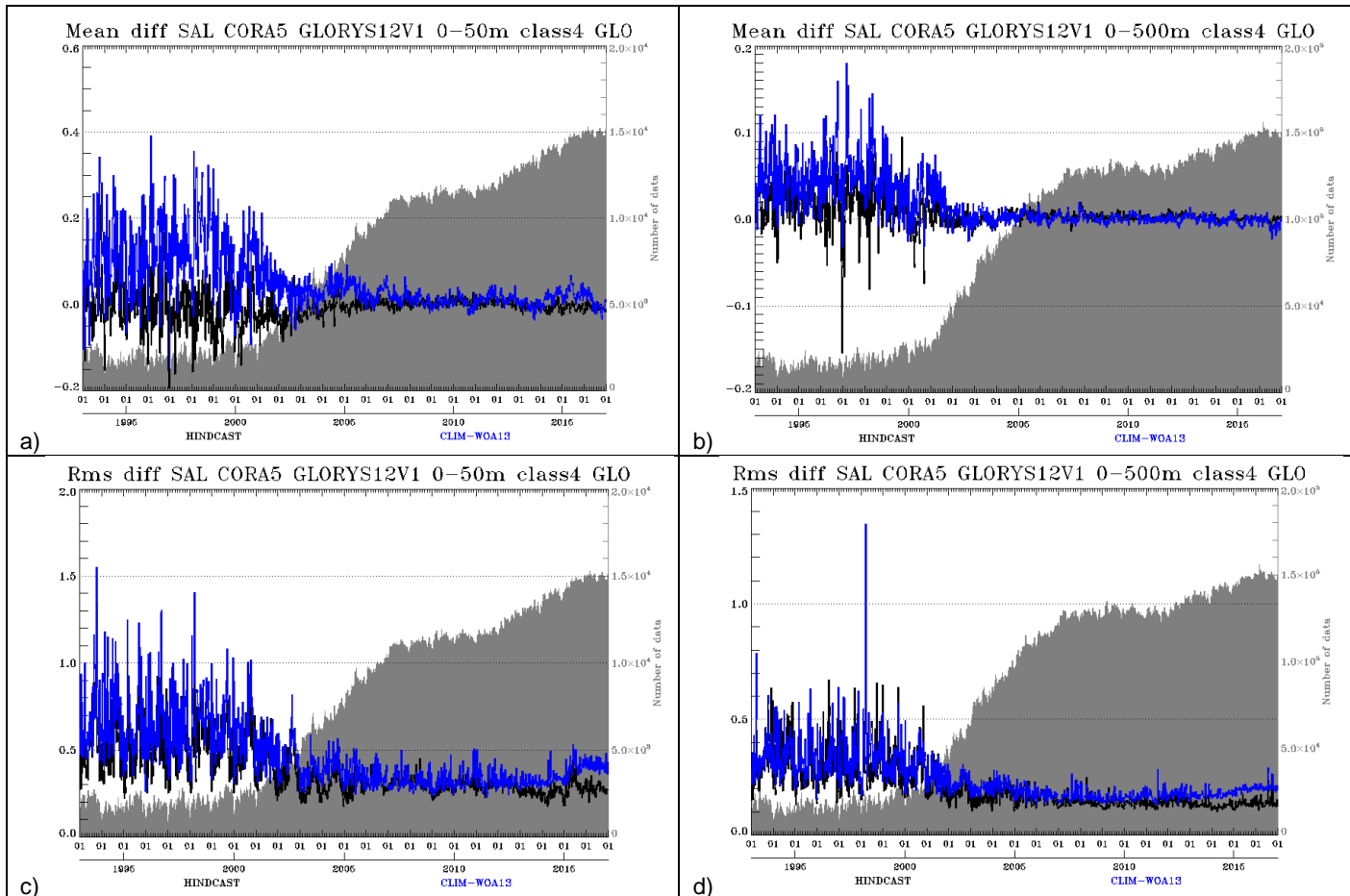


Figure 2.6.1: Timeseries (1993-2017) of mean (a, b) and RMS difference (c,d) between model Salinity and observations in black and Temperature from climatology WOA13 and observations in blue, in the 0-50 m depth layer (a, c) and 0-500 m depth layer (b, d).

As can be seen in Fig 2.6.1, the salinity scores are very stable from the 2000's. Starting from 2014, the reanalysis clearly outperforms the climatology for the bias and the RMS with low RMS differences in the 0-500 m layer depth. There is no significative bias for the surface and the 0-500 m layer.

#### IV.2.6.2 2D Maps

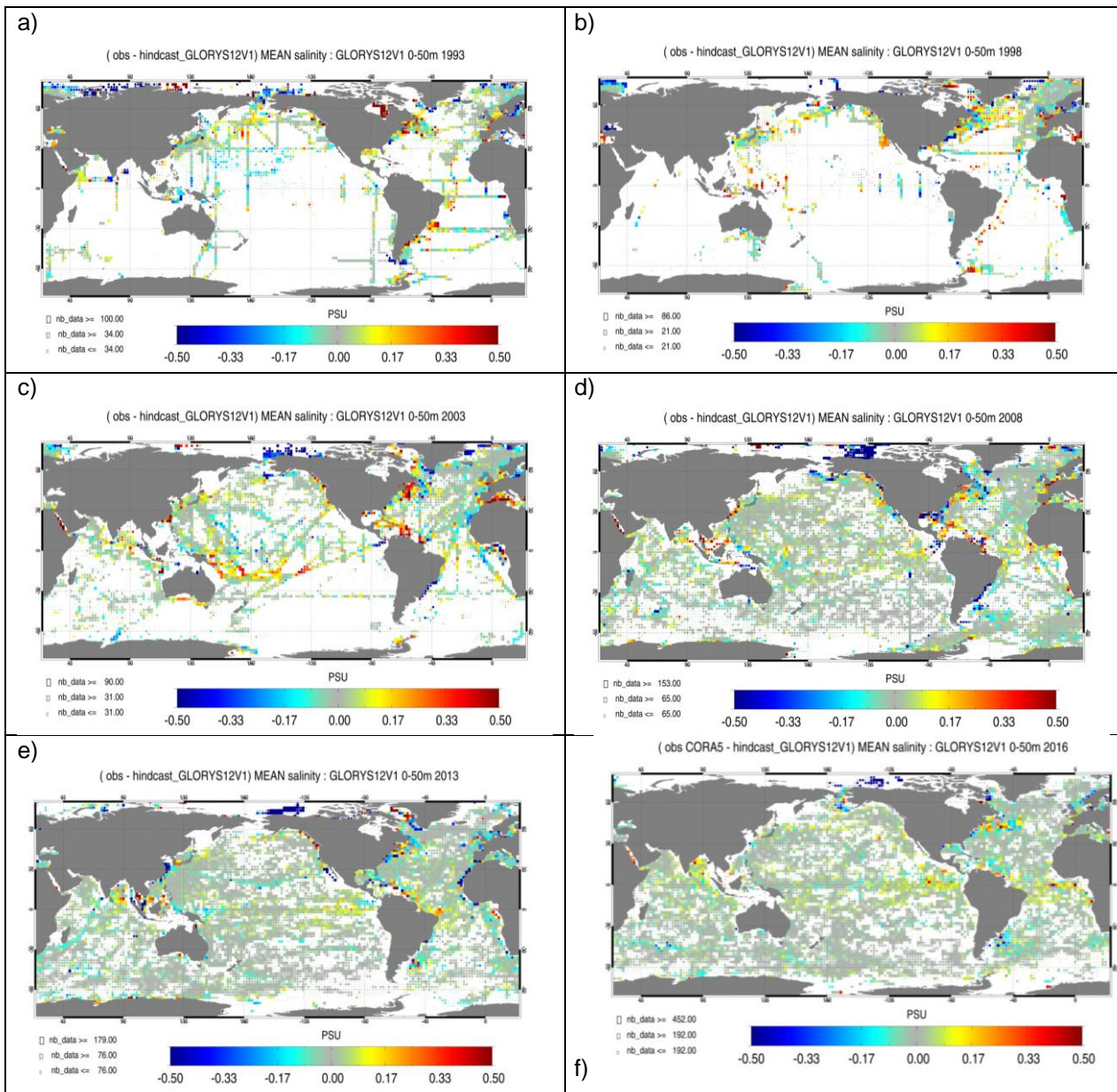


Figure 2.6.2 : Average difference Observation-Model of salinity for the years 1993 a), 1998 b), 2003 c), 2008 d), 2013 e), 2016 f) between the daily average analysis and all available T/S observations from the Cora5.0 product. The Mercator reanalysis products are taken at the time and location of the observations. Averages are performed in the 0-50 m layer and the size of the pixel proportional to the number of observations use the compute the difference in 2°x2°boxes.

At the surface (fig 2.6.2) the 2D maps exhibit a fresh bias in the East Tropical Pacific, the Atlantic tropics and the Gulf of Bengal.

**Quality Information Document  
For products  
GLOBAL\_REANALYSIS\_PHY\_001\_030**

Ref : CMEMS-GLO-QUID-001-030

Date : September 2021

Issue : 1.5

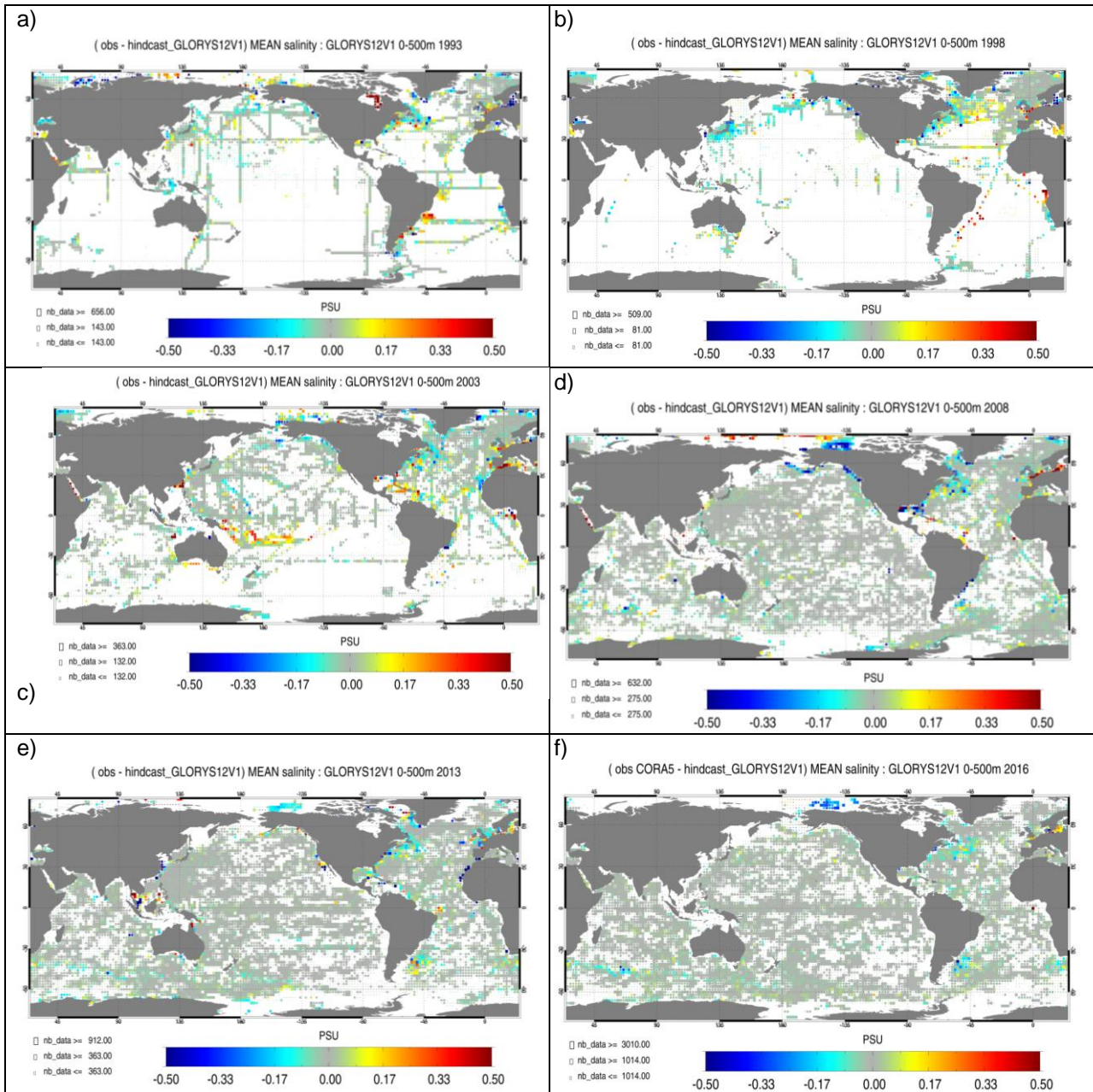


*Figure 2.6.3 : Average difference Observation-Model of salinity for the years 1993 a), 1998 b), 2003 c), 2008 d), 2013 e), 2016 f) between the daily average analysis and all available T/S observations from the Cora5.0 product. The Mercator reanalysis products are taken at the time and location of the observations. Averages are performed in the 0-500 m layer and the size of the pixel is proportional to the number of observations use the compute the difference in 2°x2°boxes.*

There is no significant bias for the salinity in the 0-500 m layer (fig 2.6.3) except a salty bias in the Beaufort Sea probably due to a bad representation of the Summer Pacific Water. There is also a salty bias in some high mesoscale activity areas like the Gulf Stream and the Zapiola region.

#### IV.2.7 S-DA-INNO-STAT

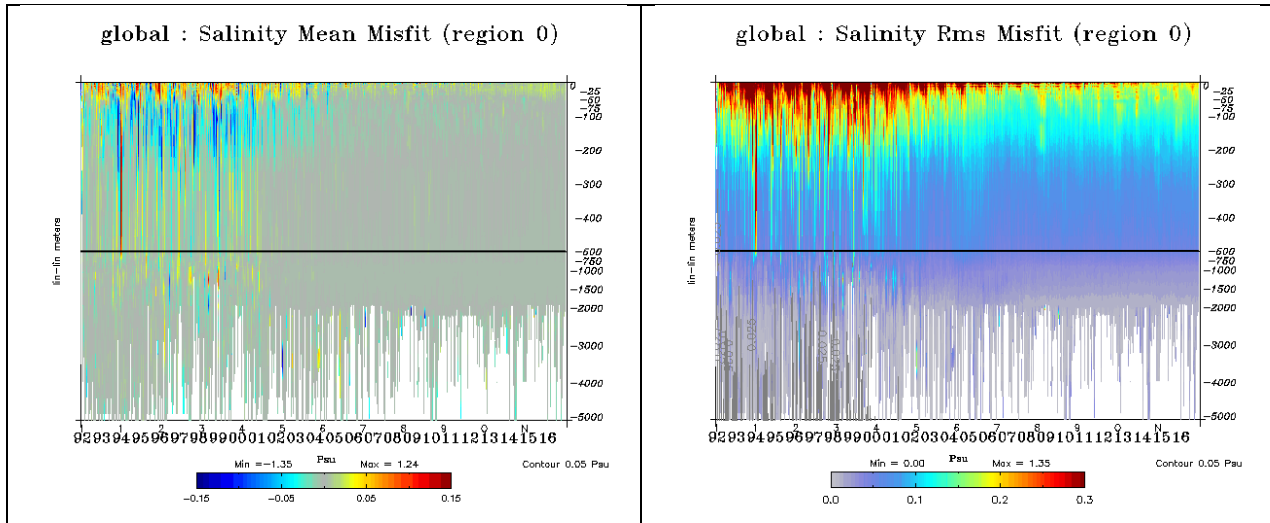


Fig 2.7: Time evolution of the domain average innovation in terms of bias (left) and RMSD (right) for CORA 4.1 in-situ salinity profiles. Covered time period: 1993 - 2015.

As can be seen in Fig 2.7 general salty bias (less than 0.1 psu) is found in the [50 m-200 m] layer, mostly during the first half of the reanalysis. The fresh bias at the surface persists throughout the reanalysis (see also section IV.2.1). Both biases and RMSD against all the in-situ observations drastically decrease with time in accordance with the increasing observations network density.

## IV.3 Currents

### IV.3.1 UV-CLASS1-15m\_MEAN

GLORYS12V1 reanalysis reproduces well the main ocean currents, as shown by the comparison with drifters velocities climatology in Fig 3.1. Strong biases appear in the western tropical Pacific, here the eastward flowing equatorial current is not reproduced by GLORYS.

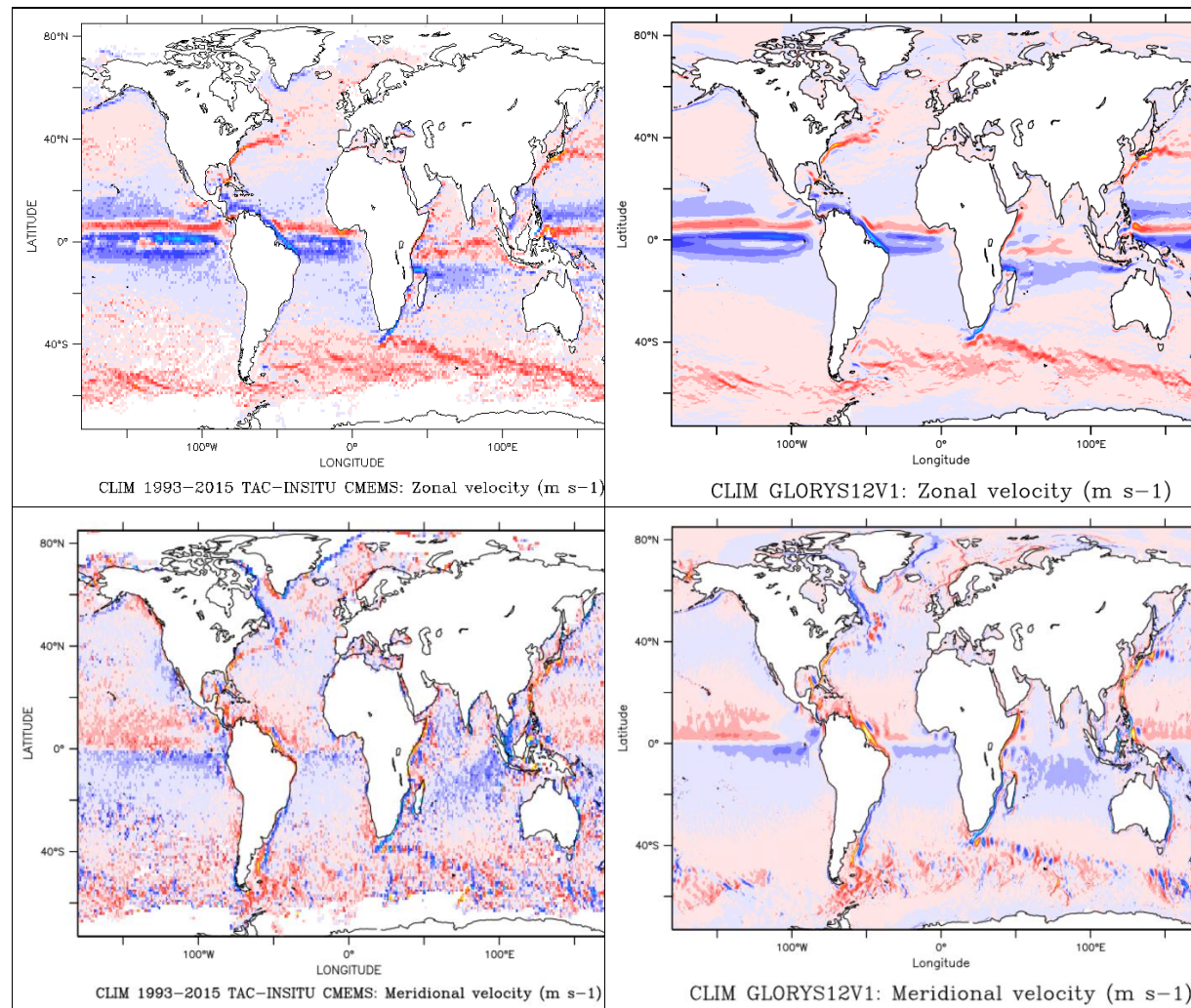


Fig. 3.1: Zonal (top) and meridional (bottom) 15 m depth current climatology for 1993-2014. NOAA AOML drifter-derived climatology from INS TAC (left) and GLORYS12V1 (right).

### IV.3.2 UV-CLASS2-MOORINGS

As seen in fig 3.2.2, the upper layers equatorial vertical dynamics structures are in good accordance with the moorings observations. The easterly surface current is however stronger in the western Pacific (probably consistent with the near surface biases in this area) and the core of the Equatorial Under Current (EUC) is weaker. RMSD are generally smaller than  $0.25 \text{ m.s}^{-1}$  in the water column with a maximum in the lower part of the EUC. Correlations with equatorial moorings also generally decrease with depth.

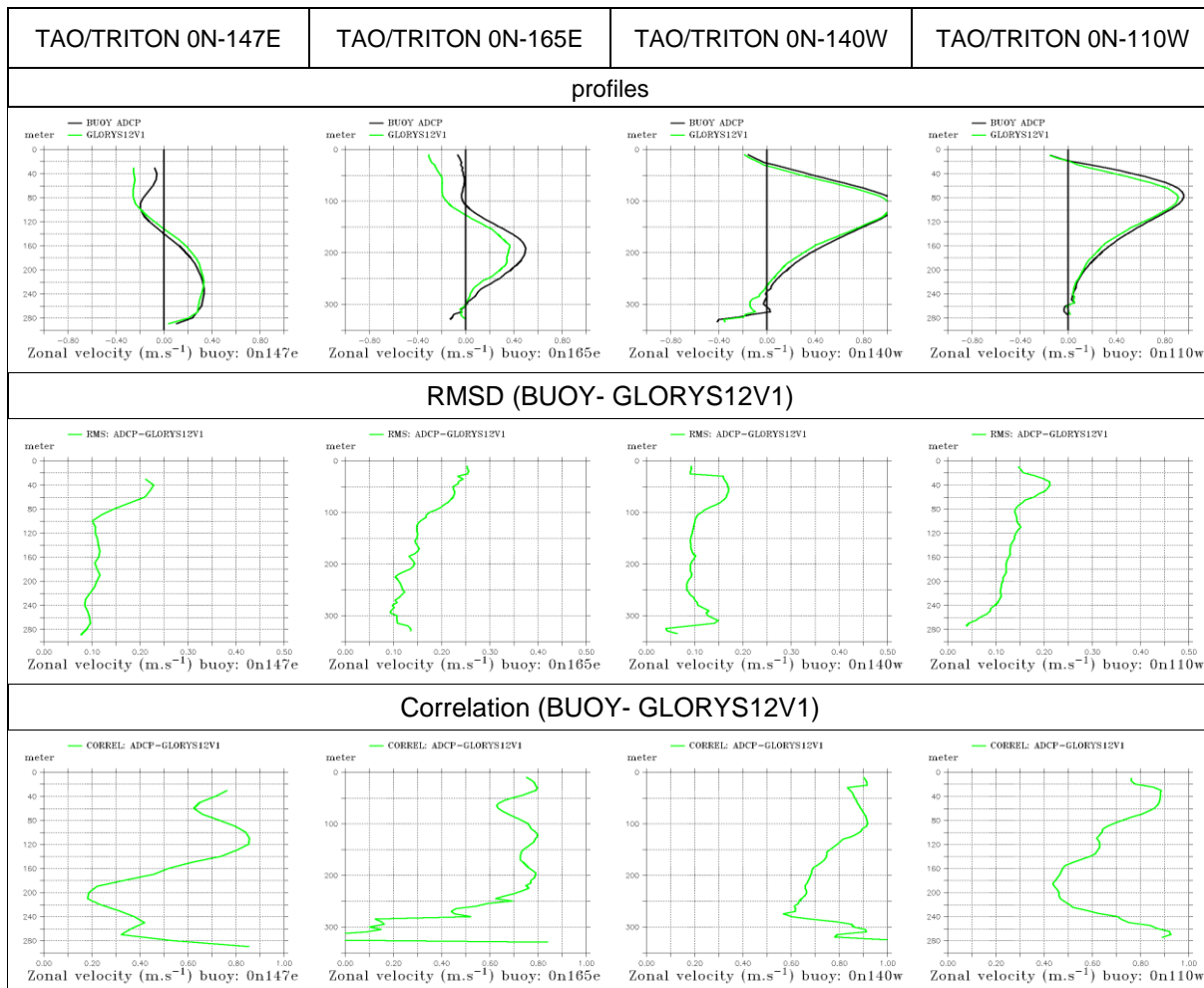


Fig. 3.2.1: Mean equatorial zonal velocity profile (top), RMSD (middle), correlation (bottom) estimated over the period 1993 – 2015 for observations (TAO/TRITON: 0N-140W, 0N-110W, 0N-165E, 0N-147E, PIRATA: 0N-23W, 0N-0E and RAMA: 0N-90E.) (black) and GLORYS12V1 (green).

**Quality Information Document  
For products  
GLOBAL\_REANALYSIS\_PHY\_001\_030**

Ref : CMEMS-GLO-QUID-001-030  
Date : September 2021  
Issue : 1.5

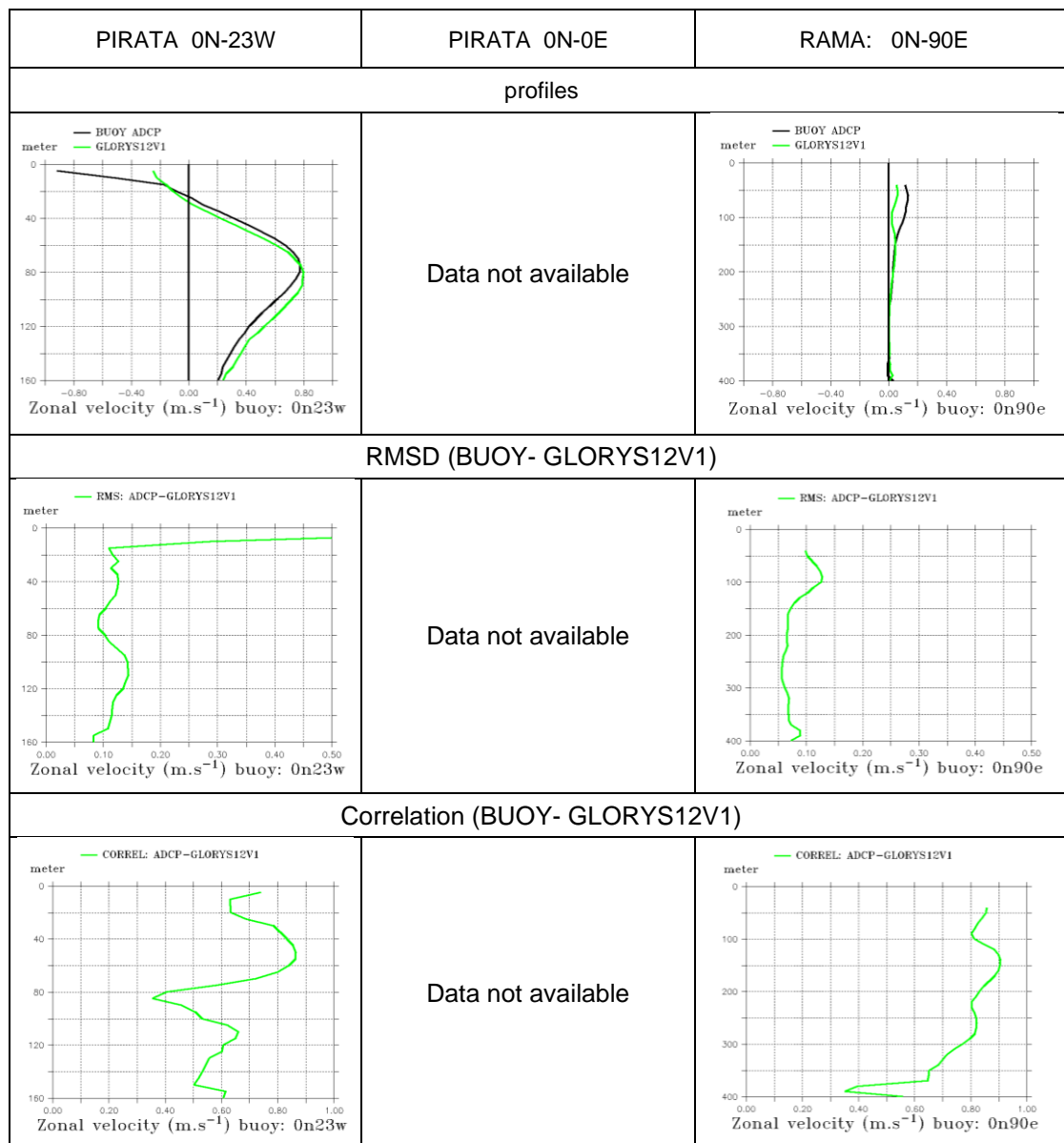


Fig. 3.2.2: Mean equatorial zonal velocity profile (top), RMSD (middle), correlation (bottom) estimated over the period 1993 – 2015 for observations (TAO/TRITON: 0N-140W, 0N-110W, 0N-165E, 0N-147E, PIRATA: 0N-23W, 0N-0E and RAMA: 0N-90E.) (black) and GLORYS12V1 (green).

### IV.3.3 UV-CLASS2-MKE\_1000m

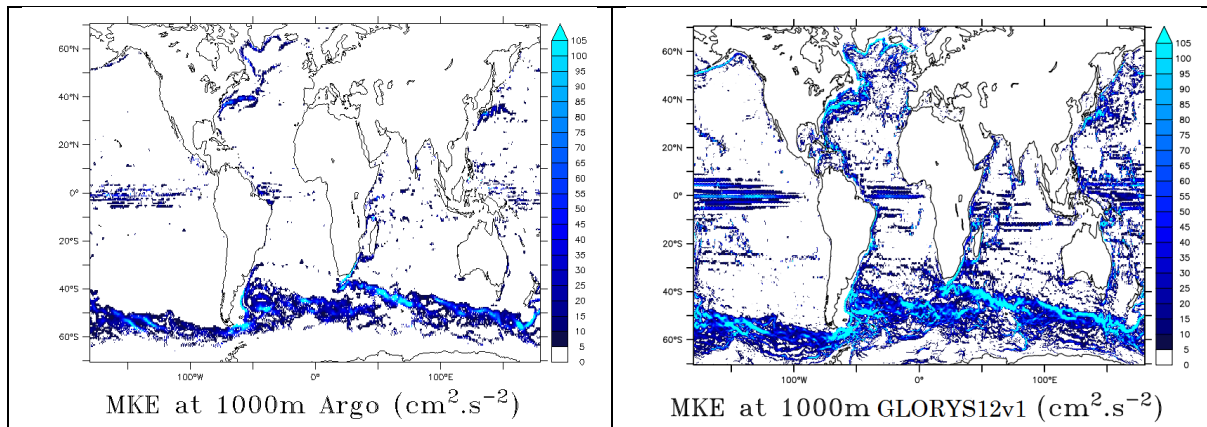


Fig. 3.3: Mean value of the kinetic energy at 1000 m from the ANDRO Argo drift data base (left) and GLORYS12V1 (right). Covered time period: 2002-2009.

The mean Kinetic Energy (MKE) at 1000 m is higher than that obtained with the ANDRO Argo drift data base all along the boundary currents and the ACC (fig 3.3). This possible overestimation of deep currents is under investigation.

## IV.4 Sea level

### IV.4.1 SL-CLASS3-2DMEAN

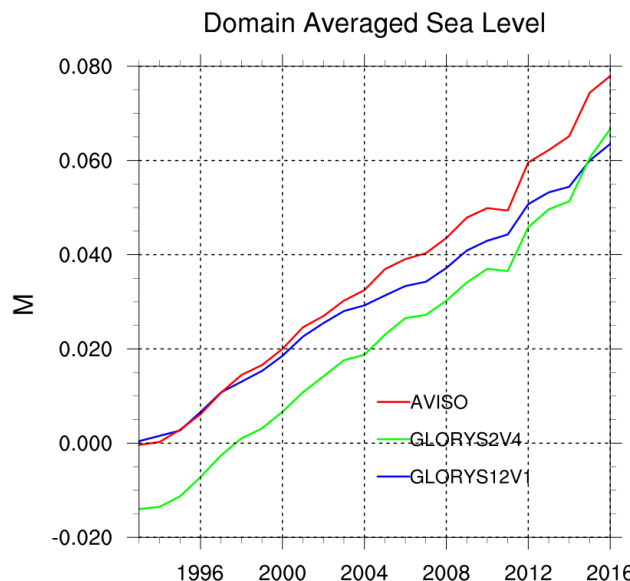


Fig. 4.1: Domain averaged sea level annual mean time series: Aviso SLA CCI observations (red), GLORYS12V1 (blue) and GLORYS2V4 (green). Covered time period is 1993-2016. The bias between AVISO data and GLORYS2V4 is due to the use of different mean sea surface height and different period of the reference

As shown in Fig 4.1, linear trends for SL-CCI, GLORYS12V1 and GLORYS2V4 reach 3.27, 2.66 and 3.3 mm/year, respectively. With 2.66 mm/year, the globally averaged sea level trend is however slightly underestimated compared to the Aviso SLA CCI observed estimates, e.g. 3.27 mm/year. Nevertheless, regional trends are particularly well reproduced by GLORYS12 (not shown, see Lellouche et al 2021). At high northern latitudes, regions not well observed by altimetry, strong sea level trends are depicted in GLORYS12V1.

#### IV.4.2 **SL-CLASS4**

Not available yet for GLORYS12V1.

#### IV.4.3 **SL-DA-INNO\_STAT**

As shown by fig 4.3 GLORYS12V1 is very close to altimetric observations and has a good ability to describe the sea level variability as the globally averaged RMSD of the forecast sea level is around 6cm. However, a bias is diagnosed, which increases during the period, reaching around 1cm (the model is lower than observations) at the end of the period.

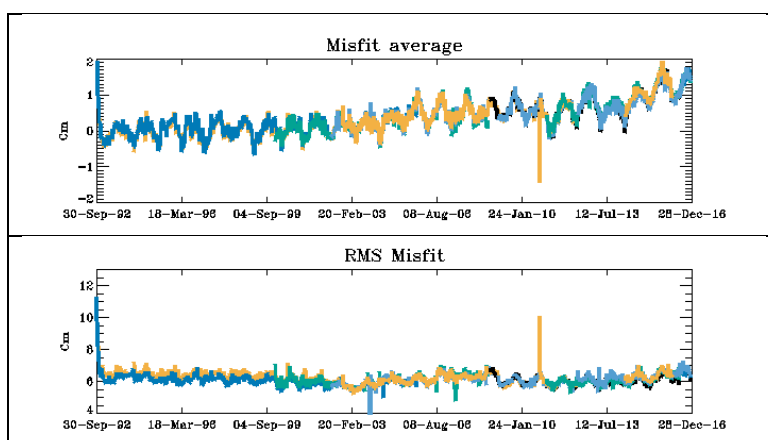


Fig. 4.3: Sea level innovation bias (top) and RMSD (bottom) over the whole domain (cm). Colours represent different altimetry satellites (ERS, T/P, Jason 1 & 2, Envisat, GFO, Saral/AltiKa, Cryosat2, HY2A). Covered time period: 1993 - 2016.

## IV.5 Transports

### IV.5.1 UV-CLASS3-VOL\_TRANSP

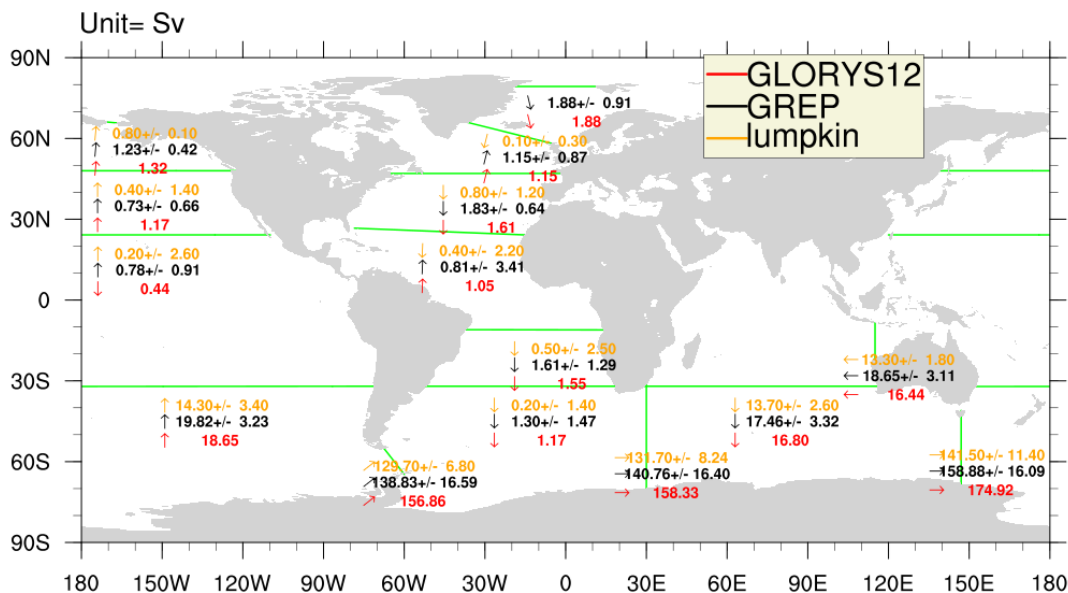


Fig 5.1 1993-2016 Mean volume transport (in Sv) for Lumpkin and Speer (2007) (orange), GREP ensemble product (black) and GLORYS12V1 reanalysis (red).

Figure 5.1 presents the 1993-2016 mean volume transports at different sections Global Ocean. Estimations for this reanalysis GLOBAL\_REANALYSIS\_PHY\_001\_030 (red) are compared to estimates from Lumpkin and Speer (2007) (orange) and from the  $\frac{1}{4}^\circ$  global reanalysis ensemble GLOBAL\_REANALYSIS-PHY-001-026 (black). GLOBAL\_REANALYSIS\_PHY\_001\_030 transports are stronger than the  $\frac{1}{4}^\circ$  ensemble.

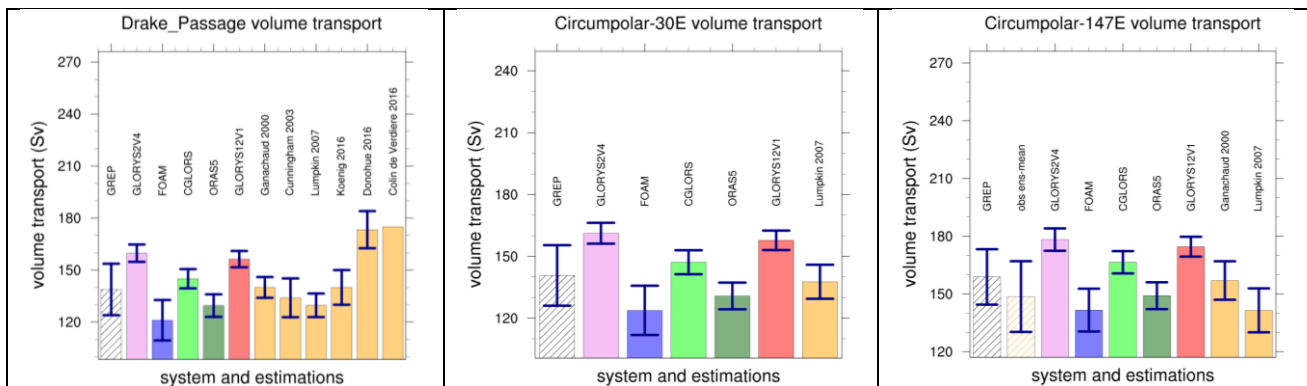


Fig 5.2 1993-2016 Mean volume transport (in Sv) estimates; from observations (orange),  $\frac{1}{4}^\circ$  reanalysis GREP (REANALYSIS-PHY-001-026 ) ensemble mean(black) and individual members( pink, blue, light green, dark green) and GLOBAL\_REANALYSIS\_PHY\_001\_030 reanalysis(red); for Drake Passage (left), Le Cap-Antarctic(middle) and Tasmania-Antarctic sections.

In Figure 5.2, we present some ACC transports from GLORYS12 and other estimations. Concerning the Drake Passage, we can see that the last estimations done by Colin de Verdière and Ollitrault, (2016) (175 Sv) and Donohue (2017) (173.3 Sv) are stronger and thus in better agreement with GLORYS12

compared to the previous estimations done by Ganachaud (2000) (140 Sv), Cunningham (2003) (134 Sv), Lumpkin and Speer (2007) (130 Sv) and Koenig (2016) (140 Sv).

#### IV.5.2 UV-CLASS3-AMOC

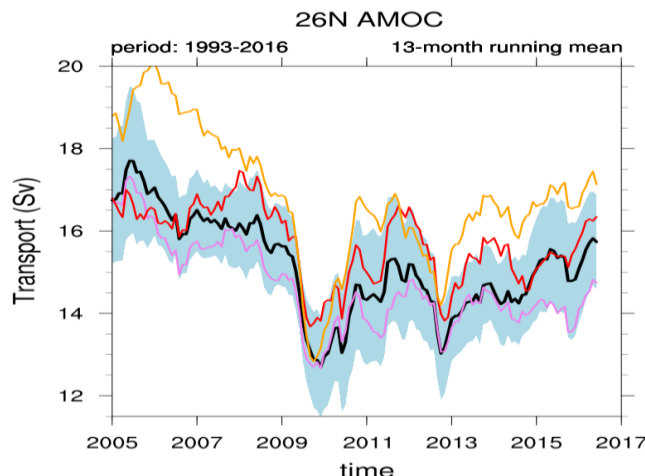


Fig 5.3: 1993-2017 26°North Meridional Overturning Current for GREP ensemble reanalysis product (black line) and GREP spread (blue shaded area), GLORYS2V4 reanalysis at  $\frac{1}{4}^\circ$  resolution (pink line), GLORYS12V1 reanalysis at  $1/12^\circ$  resolution (red line) and RAPID observation-based estimation (orange).

Figure 5.3 presents the Atlantic Meridional Overturning Current. GLOBAL\_REANALYSIS\_PHY\_001\_030\_GLOBAL\_REANALYSIS\_PHY\_001\_030 1/12° reanalysis mean value is 15.35 Sv for 200-2016 period, whereas  $\frac{1}{4}^\circ$  reanalysis GLORYS2V4 (global-reanalysis-phy-001-025) 2009-2016 mean value is 14.06 Sv; GREP ensemble of  $\frac{1}{4}^\circ$  reanalysis (REANALYSIS-PHY-001-026) mean value is 14.55 Sv. The RAPID estimate (<http://www.rapid.ac.uk/>) is 16.01 Sv.

#### IV.5.3 T-CLASS3-MHT

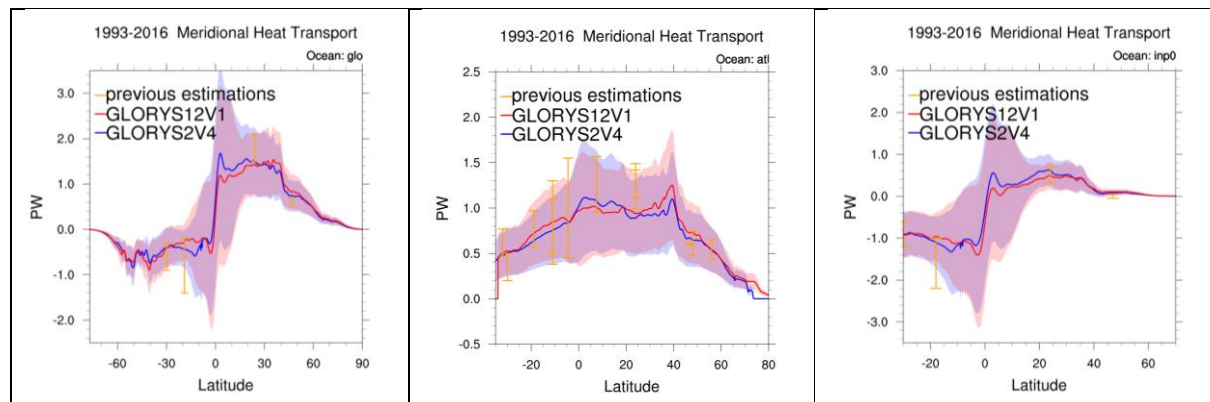


Fig 5.4: Meridional Heat Transport as a function of latitude (left: Global Ocean, middle: Atlantic Ocean, right: Indian plus Pacific Oceans) (Unit: Petawatt). Blue line and shaded area: GLORYS2V4 reanalysis at  $\frac{1}{4}^\circ$  resolution; Red line and shaded area: GLORYS12V1 reanalysis at  $1/12^\circ$  resolution; Orange: estimates provided by Ganachaud and Wunsch (2000), Trenberth and Caron (2001) (black). Covered time period: 1993 - 2016.

**Quality Information Document  
For products  
GLOBAL\_REANALYSIS\_PHY\_001\_030**

Ref :CMEMS-GLO-QUID-001-030  
Date : September 2021  
Issue : 1.5

Figure 5.4 presents the 1993-2016 Meridional Heat Transport (MHT), computed from 5-days mean fields. We compare this  $1/12^\circ$  reanalysis (GLOBAL\_REANALYSIS\_PHY\_001\_030 product, red) to the  $1/4^\circ$  reanalysis (REANALYSIS-PHY-001-026 product, blue).

$1/12^\circ$  reanalysis MHT has the same order at higher latitudes compared to the  $1/4^\circ$  reanalysis; At lower latitudes,  $1/12^\circ$  reanalysis MHT is weaker except for Atlantic basin between  $20^\circ\text{N}$  and  $40^\circ\text{N}$ .

## IV.6 Sea Ice

### IV.6.1 SI-CLASS1-CONC\_MEAN

The climatology of sea ice extent is well reproduced by GLORYS12 both in the Arctic (Fig 6.1.1) and in the Antarctic (fig 6.1.2). The sea ice concentration is overestimated in the Antarctic in September.

#### Arctic

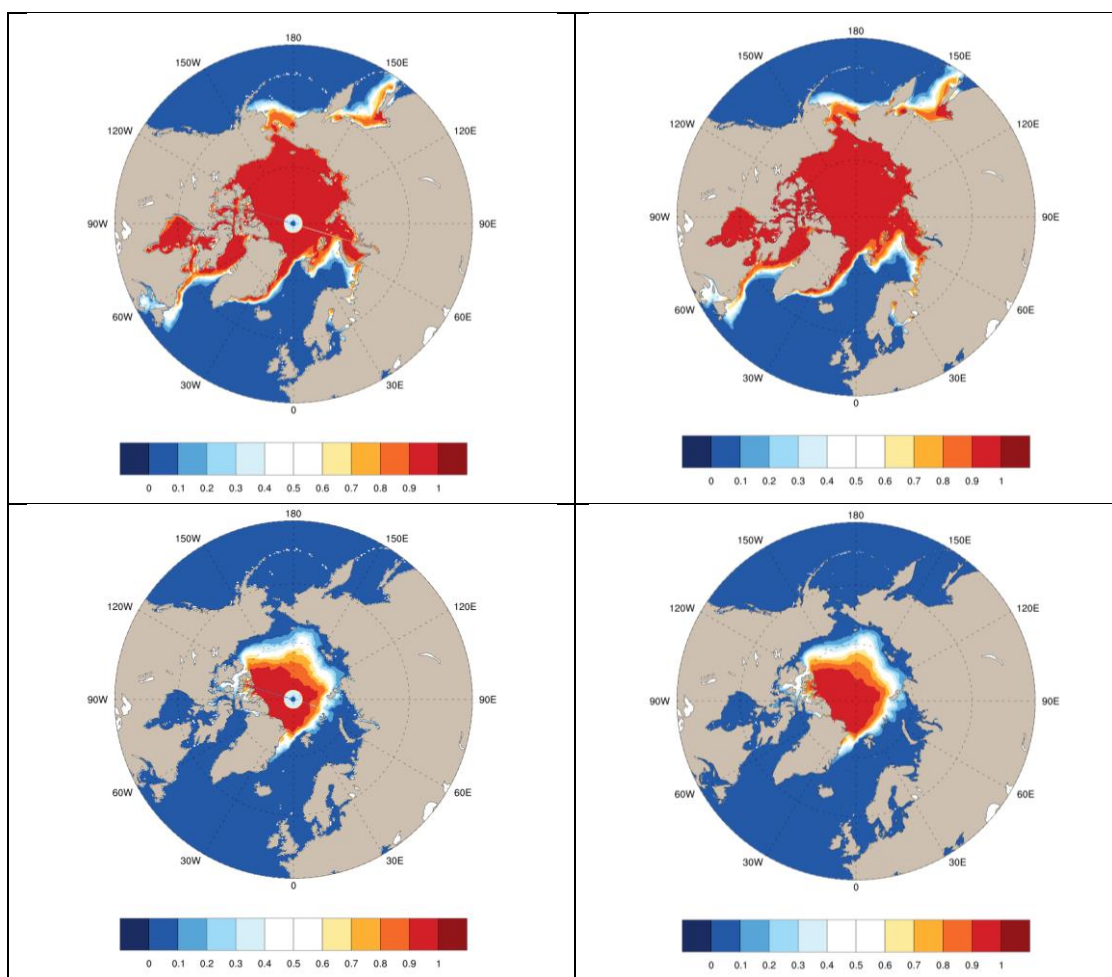


Fig 6.1.1: Arctic Sea Ice concentration climatology (in %) (1993-2016) for March (top), and September (bottom). From left to right: CERSAT observation and GLORYS12V1.

## Antarctic

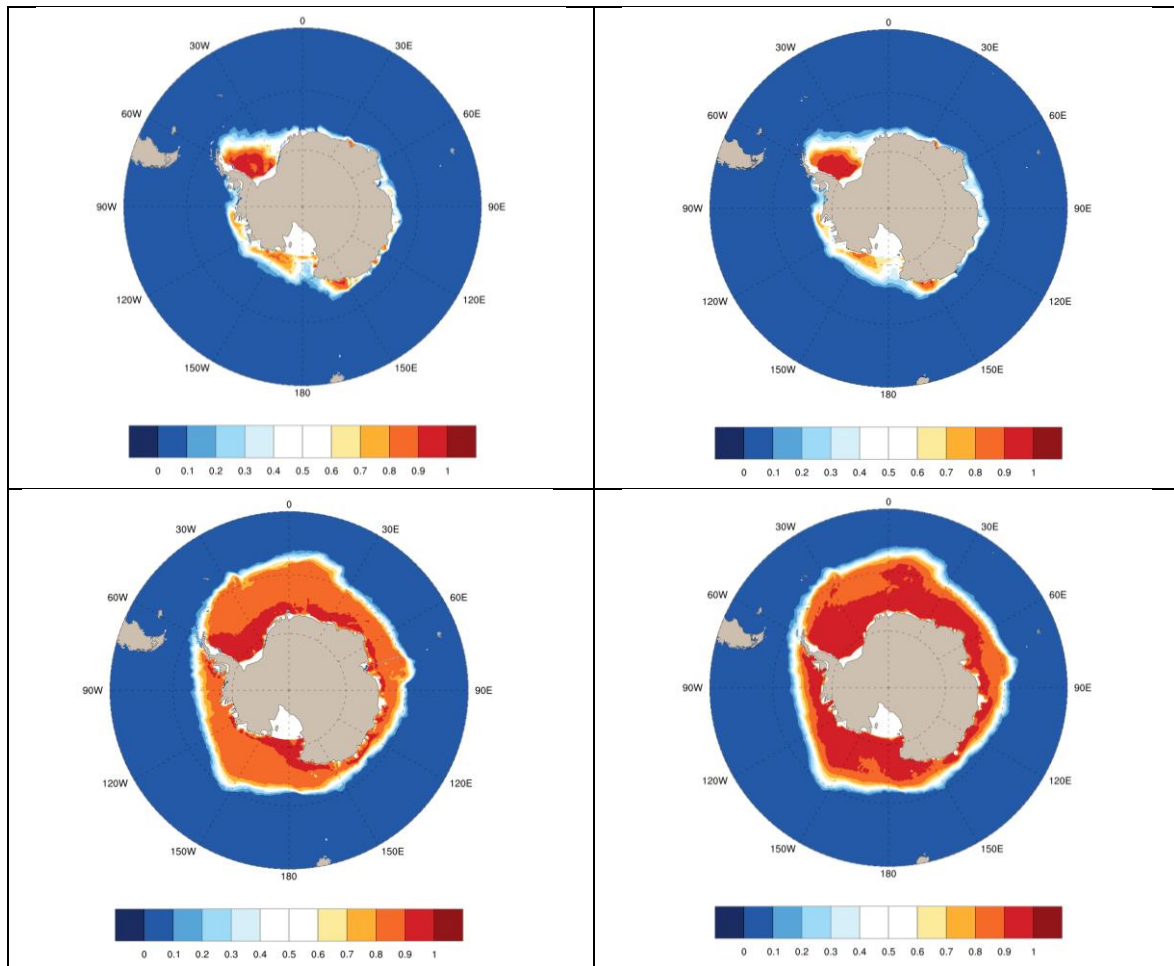


Fig 6.1.2: Antarctic Sea Ice concentration climatology (in %) (1993-2016) for March (top), and September (bottom). From left to right: CERSAT observation and GLORYS12V1.

#### IV.6.2 SI-CLASS1-CONC\_EXTREME

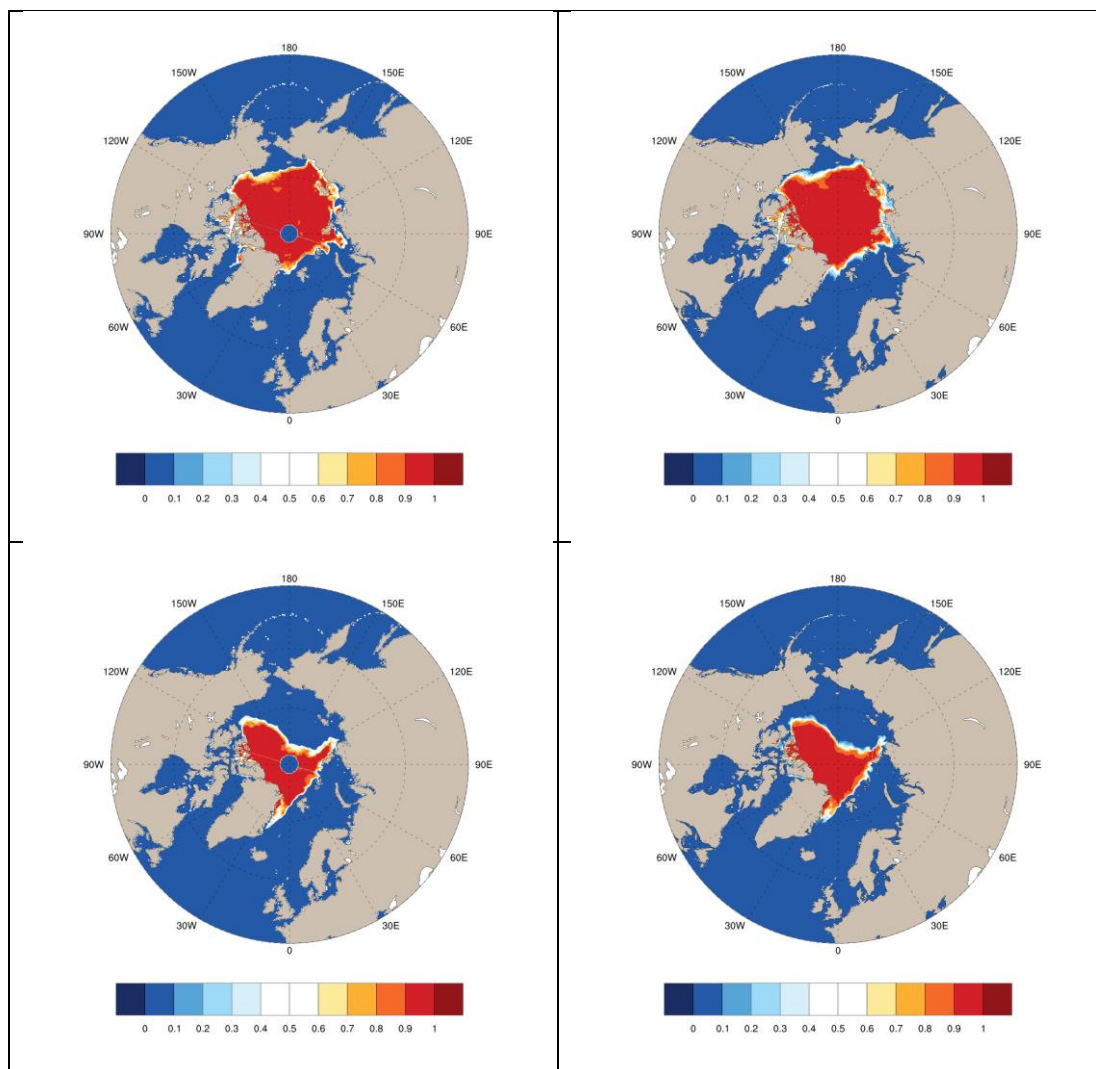


Fig 6.2: Arctic Sea Ice concentration (in %) for September 1996 (top), and September 2007 (bottom). From left to right: CERSAT observation and GLORYS12V1.

#### IV.6.3 SI-CLASS3-EXTENT

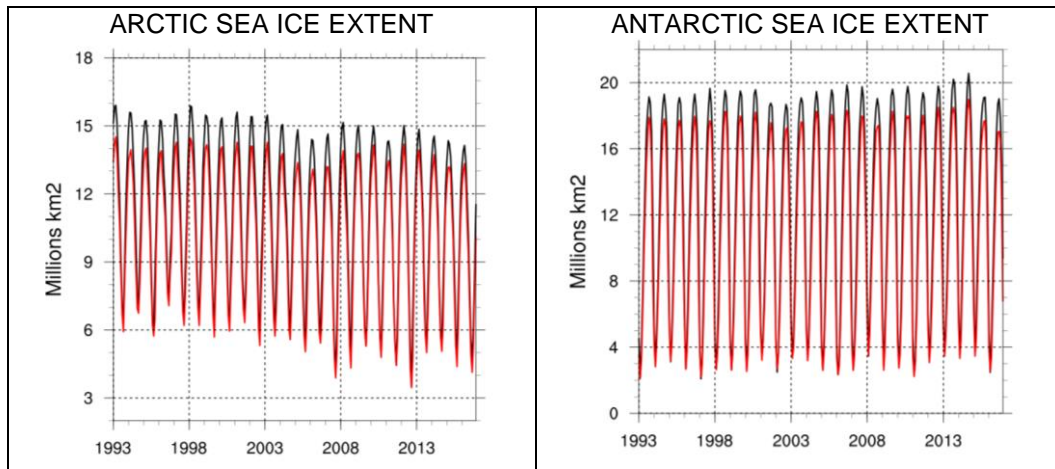


Fig 6.3: Integrated sea ice extent in the Arctic (left) and Antarctic (right) (units: $10^6 \text{ km}^2$ ). CERSAT observation (red) and GLORYS12V1 (black). Covered time period: 1993-2016.

Both Arctic sea ice extent (fig 6.3 and 6.4) and volume (fig 6.5 and 6.6) show a general decrease of respectively  $-85400 \text{ km}^2/\text{year}$  and  $-46200 \text{ km}^3/\text{year}$  for the 1993-2016 period. Both hemispheres winter sea ice extent maxima also show overestimation with the assimilated CERSAT data. Although the year 2016 exhibits an unusual strong negative anomaly, the Antarctic sea ice extent still exhibits a positive trend of  $56300 \text{ km}^2/\text{year}$  for the 1993-2016 period.

#### IV.6.4 SI-CLASS3-EXTENT\_ANO

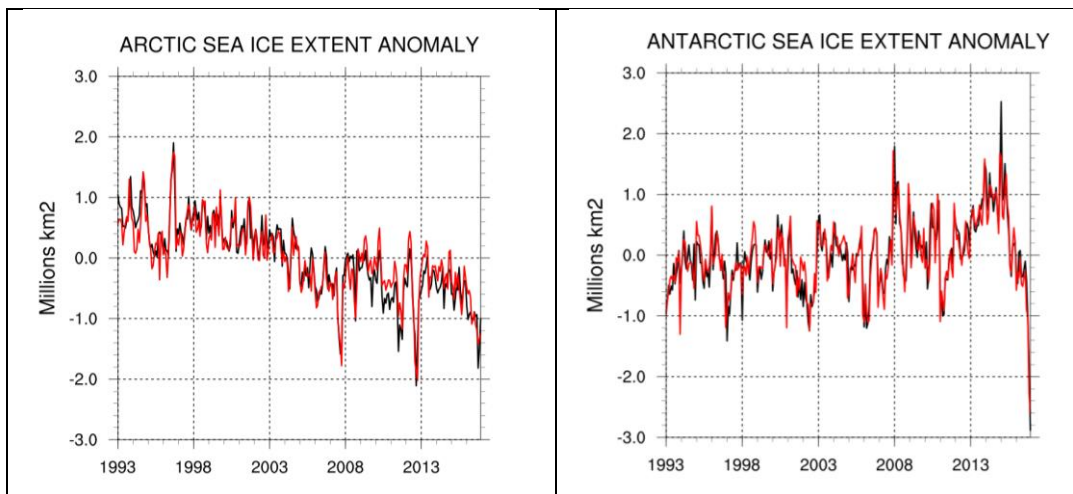


Fig 6.4: Integrated sea ice extent interannual anomalies in the Arctic (left) and Antarctic (right) (units:  $10^6 \text{ km}^2$ ). CERSAT observation (red) and GLORYS12V1 (black). The linear correlation (not de-trended) between GLORYS12V1 and CERSAT observation is respectively 0.93 and 0.91 for Arctic and Antarctic. Covered time period: 1993-2016.

#### IV.6.5 SI-CLASS3-VOL

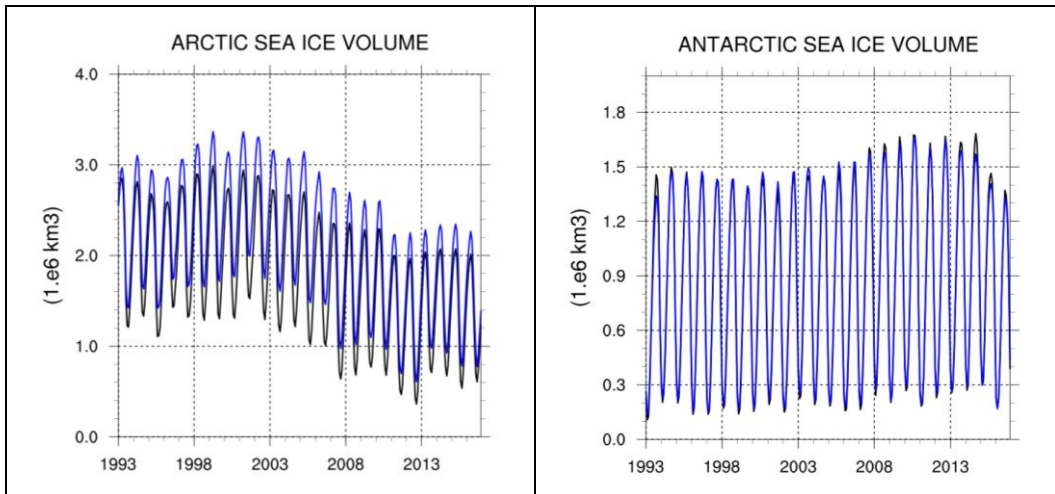


Fig 6.5: Integrated sea ice volume in the Arctic (left) and Antarctic (right) (units:  $10^6 \text{ km}^3$ ) for GLORYS12V1 (black) and GLORYS2V4 (blue). Covered time period: 1993-2016.

#### IV.6.6 SI-CLASS3-VOL\_ANO

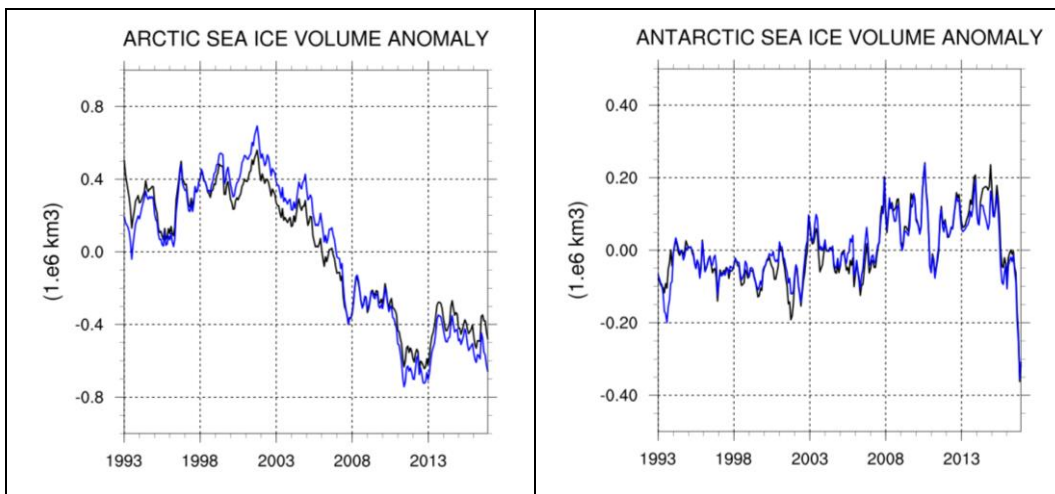


Fig 6.6: Integrated sea ice volume interannual anomalies in the Arctic (left) and Antarctic (right) (units:  $10^6 \text{ km}^3$ ) for GLORYS12V1 (black) and GLORYS2V4 (blue). Covered time period: 1993-2016.

#### IV.6.7 SI-CONC-DA-INNO-STAT

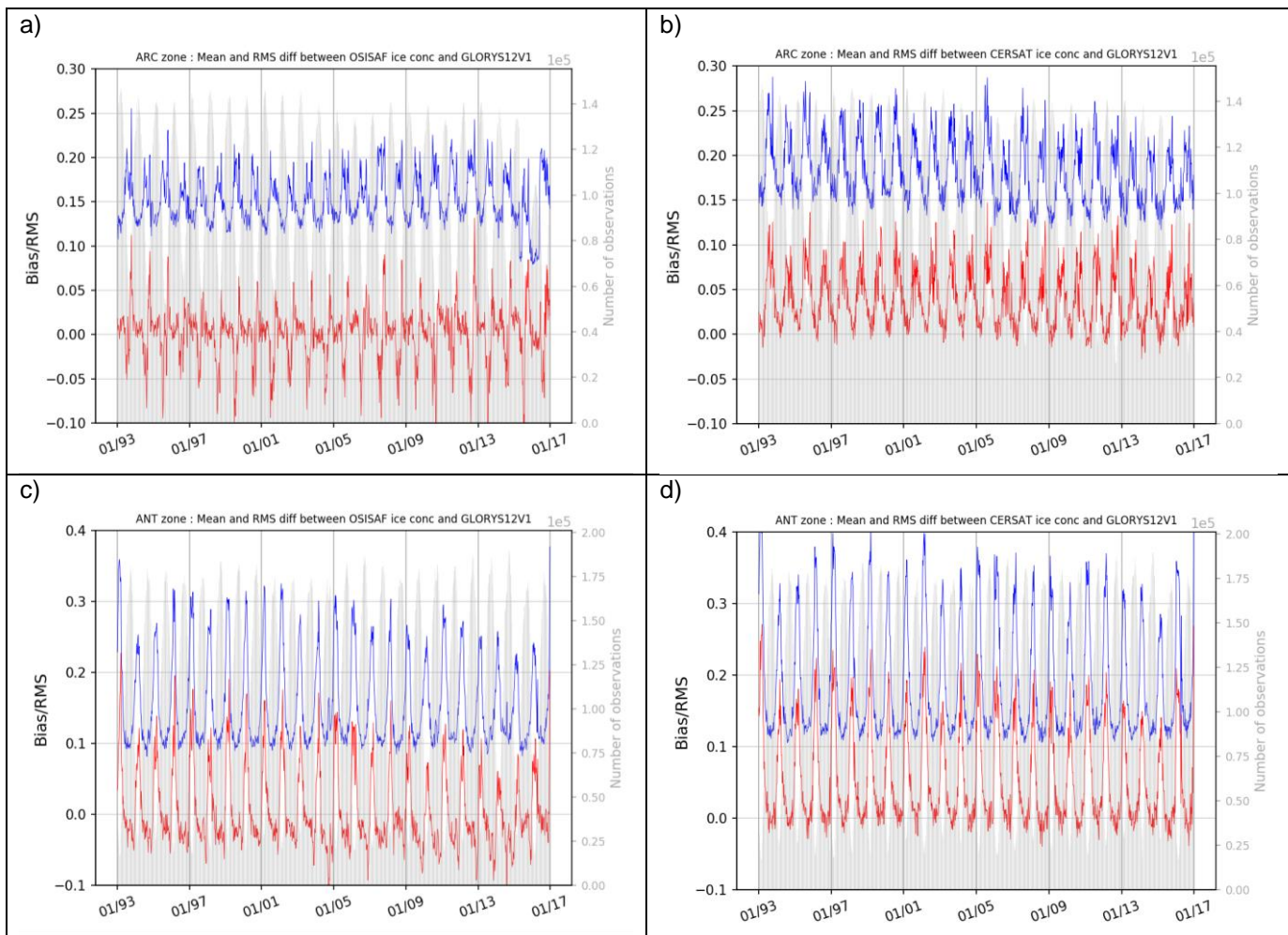


Figure 6.7: (observation-analysis) mean (red) and RMS (blue) differences of sea ice concentration (0 means no ice, 1 means 100% ice cover) in the Arctic Ocean (a and b) and Antarctic Ocean (c and d). The assimilated observations are the sea ice concentrations from CERSAT (a and c) and the independent dataset OSI TAC (b and d).

Thanks to sea ice concentration assimilation, all the sea ice extent variability (seasonal cycle, interannual variability and trend) is well reproduced in GLORYS12V1.

RMS deviations and biases with assimilated ice concentration dataset are stable all over the period (fig 6.7). For the Arctic the maximum of the RMS difference with assimilated sea ice concentration dataset reach 0.25 in the summer and 0.12 in the winter. The results are generally the same with the independent dataset but somehow higher. Positive differences between the observations and the model during spring and summer show an excess of ice melting in GLORYS12V1. During the winter the differences are positive indicating a reduced spread of ice extent. Results are similar in Antarctic with however higher RMS differences (up to 0.4 in concentration).

## **V SYSTEM'S NOTICEABLE EVENTS, OUTAGES OR CHANGES**

---

Due to the discontinuity in the production of ERA-interim atmospheric reanalysis, the forcing field used from January 2019 onwards is ERA5, this is reflected in section II.1

## **VI QUALITY CHANGES SINCE PREVIOUS VERSION**

---

This is the first version of GLORYS at 1/12°

The time extension since January 2019 may exhibit quality differences due to the use of ERA5, see section II.1.

## VII REFERENCES

---

- Colin de Verdière, A., & Ollitrault, M. (2016). A direct determination of the World Ocean barotropic circulation. *Journal of Physical Oceanography*, 46(1), 255-273.
- Donohue, K. A., Tracey, K. L., Watts, D. R., Chidichimo, M. P., & Chereskin, T. K. (2016). Mean antarctic circumpolar current transport measured in drake passage. *Geophysical Research Letters*, 43(22), 11-760.
- Drevillon et al (2018) Report on validation guidelines for ocean reanalyses of the Copernicus Marine Environment Monitoring Service, CMEMS-RAN-ScV-common-plan
- Ganachaud, A., & Wunsch, C. (2000). Improved estimates of global ocean circulation, heat transport and mixing from hydrographic data. *Nature*, 408(6811), 453-457.
- Gouretski, V.V. and Koltermann, K.P.: Woce global hydrographic climatology. Technical Report 35/2004, Berichte des Bundesamtes für Seeschifffahrt und Hydrographie, 2004.
- Lellouche, J.-M., Greiner, E., Le Galloudec, O., Garric, G., Regnier, C., Drevillon, M., et al. (2018). Recent updates on the copernicus marine service global ocean monitoring and forecasting real-time 1/12° high resolution system. *Ocean Sci.* 14, 1093–1126. doi: 10.5194/os-14-1093-2018
- Jean-Michel, L., Eric, G., Romain, B.-B., Gilles, G., Angélique, M., Marie, D., et al. (2021). The Copernicus Global 1/12° Oceanic and Sea Ice GLORYS12 Reanalysis. *Frontiers in Earth Science* 9, 585. doi:10.3389/feart.2021.698876.
- Lumpkin, R., & Speer, K. (2007). Global ocean meridional overturning. *Journal of Physical Oceanography*, 37(10), 2550-2562.
- Trenberth, K. E., & Caron, J. M. (2001). Estimates of meridional atmosphere and ocean heat transports. *Journal of Climate*, 14(16), 3433-3443.
- Koenig, Z., Provost, C., Park, Y. H., Ferrari, R., & Sennéchal, N. (2016). Anatomy of the Antarctic Circumpolar Current volume transports through Drake Passage. *Journal of Geophysical Research: Oceans*, 121(4), 2572-2595.